Resonance Raman, CARS, and Picosecond Absorption Spectroscopy of Copper Porphyrins: The Evidence for the Exciplex Formation with Oxygen-Containing Solvent Molecules

ARTICLE *in* THE JOURNAL OF PHYSICAL CHEMISTRY · MARCH 1995

DOI: 10.1021/j100010a006

5 AUTHORS, INCLUDING:

Sergei G Kruglik
Pierre and Marie Curie University - Paris 6
99 PUBLICATIONS **919** CITATIONS
SEE PROFILE

P.A. Apanasevich
Stepanov Institut of Physics of National Acad…
97 PUBLICATIONS **394** CITATIONS
SEE PROFILE

V.s. Chirvony
University of Valencia
43 PUBLICATIONS **361** CITATIONS
SEE PROFILE

Valentin Antonovich Orlovich
National Academy of Sciences of Belarus
181 PUBLICATIONS **1,044** CITATIONS
SEE PROFILE

Resonance Raman, CARS, and Picosecond Absorption Spectroscopy of Copper Porphyrins: The Evidence for the Exciplex Formation with Oxygen-Containing Solvent Molecules

Sergei G. Kruglik,*,† Pavel A. Apanasevich,† Vladimir S. Chirvony,*,‡ Vladimir V. Kvach,† and Valentin A. Orlovich†

B. I. Stepanov Institute of Physics, Academy of Sciences of Belarus, 70 F. Skaryna Avenue, Minsk 220072, Republic of Belarus, and Institute of Molecular and Atomic Physics, Academy of Sciences of Belarus, 70 F. Skaryna Avenue, Minsk 220072, Republic of Belarus

Received: February 3, 1994; In Final Form: September 27, 1994⊗

The reversible process of photoinduced binding of oxygen (O)-containing solvent molecules by copper (Cu)−porphyrins has been observed and studied in detail by the methods of resonance Raman (RR), resonance coherent anti-Stokes Raman scattering (RCARS), and picosecond absorption spectroscopy. It was found that the formation of the excited complex (exciplex) [(CuP)*−L] occurs when an O-containing molecule L is attached as an axial ligand to a Cu−porphyrin in the excited tripdoublet−quartet state manifold $^{2,4}T_1$. If L is a molecule of tetrahydrofuran (THF), dioxane, or cyclohexanone, then the deactivation of the excitation energy inside the five-coordinate Cu−porphyrin proceeds via the low-lying excited (d,d) state, which involves the promotion of an electron from the highest filled d_{z^2} orbital to the half-filled $d_{x^2-y^2}$ orbital. This state is displayed prominently in transient RR and RCARS spectra by large frequency shifts in selected metalloporphyrin marker lines and in transient difference absorption spectra by characteristic derivative-like absorption changes. The decay of the excited (d,d) state having a lifetime of hundreds of picoseconds is accompanied by the exciplex disruption into initial components. Saturation RCARS studies reveal the existence of the second exciplex deactivation channel, presumably involving the low-lying excited intramolecular charge-transfer (CT) state of the Cu−porphyrin, which is competitive with the decay pathway via the (d,d) state. It was found that for some axial ligands (L = dimethyl sulfoxide (DMSO), dimethyl formamide (DMF)) this relaxation channel via the CT state dominates. The vibrational analysis of transient Raman spectra is done to elucidate the structural changes of five-coordinate Cu−porphyrins occurring both in the excited (d,d) state at ambient temperature and in the ground electronic state, being stable at liquid nitrogen temperature (77 K).

Introduction

Cu−porphyrins ($3d^9$ metal ion configuration) are an interesting photophysical object for investigations,[1−16] since they are a kind of boundary between luminescent closed-shell metalloporphyrins and nonluminescent complexes whose d-shells of the central metal vary from $3d^4$ to $3d^8$. Indeed, Cu−porphyrins do not exhibit fluorescence (quantum yield $< 10^{-5}$) but display rather moderately strong phosphorescence. The effect of one unpaired electron in the outer $d_{x^2-y^2}$ orbital of copper determines the complicated structure of the low-lying excited electronic states. As a result of coupling of this d electron with π electrons of the conjugated porphyrin macrocycle, the ground and singlet excited $^1(\pi,\pi^*)$ states become doublet or, using the terminology of Gouterman,[2] singdoublet $^2S_0$ and $^2S_1(\pi,\pi^*)$ respectively, whereas the excited triplet $^3(\pi,\pi^*)$ state is split into a tripdoublet $^2T_1(\pi,\pi^*)$ and a tripquartet $^4T_1(\pi,\pi^*)$.[2,3]

The relaxation processes in excited Cu−porphyrins have been extensively studied by picosecond transient absorption spectroscopy.[4−9] It was found that the photoexcitation of a Cu−porphyrin in the $^2S_0 \rightarrow {}^2S_n$ channel is followed by the extremely fast ($\tau < 1$ ps) intersystem crossing to the excited $^2T_1$ state, hindering porphyrin fluorescence. Establishment of the equilibrium between the $^2T_1$ and $^4T_1$ states proceeds within hundreds of picoseconds. Note that splitting between the excited $^2T_1$ and $^4T_1$ states for different Cu−porphyrins varies within dozens to hundreds of cm^{-1}, depending on the porphyrin structure.[3a,10−12]

For the sake of simplicity, we shall use further the conventional designation of the triplet state T_1 for the "tripmultiplet" state in the case when the state of multiplicity is not essential. For example, transient absorption spectra from the triplet manifold will be denoted triplet−triplet (π,π^*) absorption. Following electronic excitation, decay from the triplet manifold to the ground state normally occurs through nonradiative pathways. The relaxation times of this process are of dozens to hundreds of nanoseconds at room temperature in noncoordinating solvents such as benzene, toluene, etc. At 77 K, Cu−porphyrins display phosphorescence from the $^2T_1 \rightarrow {}^2S_0$ channel, which, however, is strongly quenched at room temperature.

Besides (π,π^*) transitions, two intramolecular CT transitions between π orbitals of the porphyrin and d orbitals of the metal ((d,π^*) and (π,d) transitions) are possible which play an important role in various photophysical processes in Cu−porphyrins. According to Kim et al.,[7] it is the nonluminescent, thermally accessible CT state lying not too far above the $^{2,4}T_1$ state that causes Cu−porphyrins' phosphorescence quenching at room temperature. At the same time, Asano et al.[13] explained the relaxation processes taking place in the excited states of Cu−porphyrins in noncoordinating solvents at both room and lowered temperatures without using the hypothesis about the CT state influence.

The set of possible low-lying excited states of Cu−porphyrins would be incomplete without including the excited (d,d) state, arising from the promotion of one electron from the filled metal d_{z^2} orbital to the half-filled $d_{x^2-y^2}$ orbital. Iterative extended Hückel (IEH) calculations by Shelnutt and Gouterman on Cu−porphyrin ligation[7,14] revealed that binding of the water molecule

* Authors to whom correspondence should be addressed.
† B. I. Stepanov Institute of Physics.
‡ Institute of Molecular and Atomic Physics.
⊗ Abstract published in *Advance ACS Abstracts,* February 15, 1995.

0022-3654/95/2099-2978$09.00/0

as an axial ligand causes significant lowering of the $^2[d_{z^2},d_{x^2-y^2}]$ state, and the lowest position calculated ($E_{d-d} \approx 1.7$ eV) is characteristic of the five-coordinate complex with a domed structure.

Our current interest in Cu−porphyrins is caused by their ability to participate in the reactions of photoinduced attachment of axial ligands to the central copper ion; the reactions which model various native biological processes. Indeed, the reversible dark processes of axial binding/release of extra ligands by iron porphyrin complexes, being the active centers of a wide class of heme proteins and enzymes, are of prime biological interest and provide such important functions as molecular oxygen transport and storage (hemoglobin and myoglobin), electron transfer (cytochrome), etc. For studying the initial ultrafast stages of these biological processes and for modeling them by the corresponding binding/release photoreactions, various molecular axial ligands and various porphyrin complexes with transition metals having low-lying d orbitals (Fe, Co, Ni, Cu) have been used.[4] Such modeling is valid because in these complexes the same types of d orbitals are involved in the processes of excitation relaxation which are responsible for the dark binding and release of the axial ligands in the above-mentioned biological systems.

For Cu−porphyrins, until recently only one complexation process has been discovered and studied: the reversible photoinduced coordination of the molecules of nitrogen (N) bases (piperidine, pyridine, pyrrolidine) to a four-coordinate copper ion as a fifth axial ligand.[6−8,14,15] It has been shown that this process may occur both in the ground and in the excited electronic states. In both cases, complexation with a N-containing molecule causes very fast radiationless decay of the triplet (π,π^*) states; the lifetimes observed for these triplet states (10−150 ps) are 3 orders of magnitude shorter than the lifetime of the Cu−porphyrin triplet state in noncoordinating solvents. The effect is attributed to a lower energy gap between the CT and T_1 states for five-coordinate Cu−porphyrins and can be described as follows.[7] The attachment of the copper ion to a nitrogen base as an axial ligand perturbs the porphyrin molecular orbitals and causes a lowering of the energy for the CT state. The observed fast single-exponential kinetics of triplet-state depopulation is explained as a radiationless relaxation to the ground electronic state via the lowered CT state. This interpretation requires that the relaxation from the CT to the ground state is extremely fast, since spectral manifestations of the CT-state population have not been observed on the picosecond time scale. Another possible explanation of the lack of direct spectral manifestations of the CT state is that this state indirectly participates in the quenching process as a factor of "mixing" of the states $^{2,4}T_1$ and $^2S_0$. Concerning the nature of this intermediate excited state, IEH calculations found that most probably it is a $^2[a_{2u}(\pi),d_{x^2-y^2}]$ state arising from the transferring of electronic density from the highest occupied molecular orbital a_{2u} to the half-filled metal orbital $d_{x^2-y^2}$.[7,14]

Previously,[16] we have observed another reversible photochemical reaction with the participation of Cu−porphyrins, namely, the photoinduced ligation of Cu−porphyrins by O-containing molecules of organic bases. This paper summarizes the results of studies of various Cu−porphyrins and O-containing solvents carried out using different spectroscopic techniques. The rates and relaxation channels of photoexcitation were investigated by picosecond transient absorption spectroscopy. However, this technique examines directly the electronic changes in the system, providing only indirect information on the geometric changes of the molecule in the excited state. The application of spontaneous and coherent Raman techniques using nanosecond laser pulses has made it possible to obtain transient Raman spectra which provide information about the structural distortions of a porphyrin skeleton in the excited electronic state under high-power irradiation. In the paper, we present spectroscopic evidence for the photoinduced formation of the excited complex (exciplex) between a Cu−porphyrin and an O-containing solvent molecule attached to the metal as an axial ligand. Comprehensive studies on the kinetics and mechanism of the reaction as well as on deactivation pathways have been performed. It is proved that the low-lying excited (d,d) state plays crucial role, either dominating or effectively competing with the earlier predicted excited CT state in deactivating the exciplex. Structural changes caused by axial ligation are also discussed for five-coordinate Cu−octaethylporphyrin (OEP) both in the excited (d,d) state of the exciplex [$(CuOEP)^*_{d,d}$−THF] at ambient temperature and in the ground state of the complex [CuOEP−THF], being stable at 77 K. It is found that the exciplex species exhibits both expansion of the porphyrin core and removal of the central metal out of the macrocycle plane, producing of the doming structure. Furthermore, the electron density donation from the oxygen p_z orbital of the ligand molecule to the d orbitals of the central metal is revealed by the large-frequency downshift of the ν_4 marker line. In contrast, the low-temperature Raman study gave experimental evidence that binding of a THF molecule as an axial ligand in the ground state stabilizes the planar structure of CuOEP at liquid nitrogen temperature, while the noncomplexed CuOEP species exists in the ruffled form.

Experimental Section

The Raman spectrometer was built on the basis of a home-made pulsed Nd:YAG laser with pulse duration 10 ns and repetition rate 12.5 Hz.[17] For Soret excitation, the following wavelengths were used: (a) radiation in the 390−405 nm range resulting from the process of frequency summation of the first harmonic of the YAG fundamental with the radiation of a narrow-band dye laser; (b) radiation at the wavelength 416 nm—the first Stokes component of stimulated Raman scattering (SRS) of the third harmonic of the YAG fundamental in compressed hydrogen at 1000 psi;[18] (c) radiation at the wavelength 436 nm—the first anti-Stokes component of SRS of the YAG second harmonic in compressed hydrogen at 800 psi.

To create a significant population of the excited states of the molecules being investigated, besides the above-mentioned laser sources we have also used "pump" radiation at the wavelengths 532 nm (YAG second harmonic) and 560 nm (Rhodamine 6G dye laser radiation), falling in resonance with the Q bands of metalloporphyrin absorption.

All Raman spectra were collected using a backscattering geometry and were dispersed by a double diffraction monochromator. Laser radiation was focused near the front surface of the sample cell by a cylindrical lens ($f = 25$ cm, illuminated area of ca. 1×5 mm^2) when Raman spectra at low excitation power were recorded. High excitation power was provided by sharp focusing using a spherical lens ($f = 25$ cm, beam spot diameter was varied from 1 to 0.1 mm). The Raman analog signal obtained from the photomultiplier at each laser shot was processed and digitized by a rapid stroboscopic voltmeter (strobe pulse duration 4 ns) and then recorded in a PC.

For excitation into the Q band, the vibrational structure of Cu−porphyrins was investigated using a coherent Raman spectrometer based on nanosecond Nd:YAG and independently tuned one or two narrow-band dye lasers. To obtain the best quality of resonance coherent anti-Stokes Raman scattering (RCARS) spectra, we implemented the method of polarization suppression of the nonresonant coherent background, caused

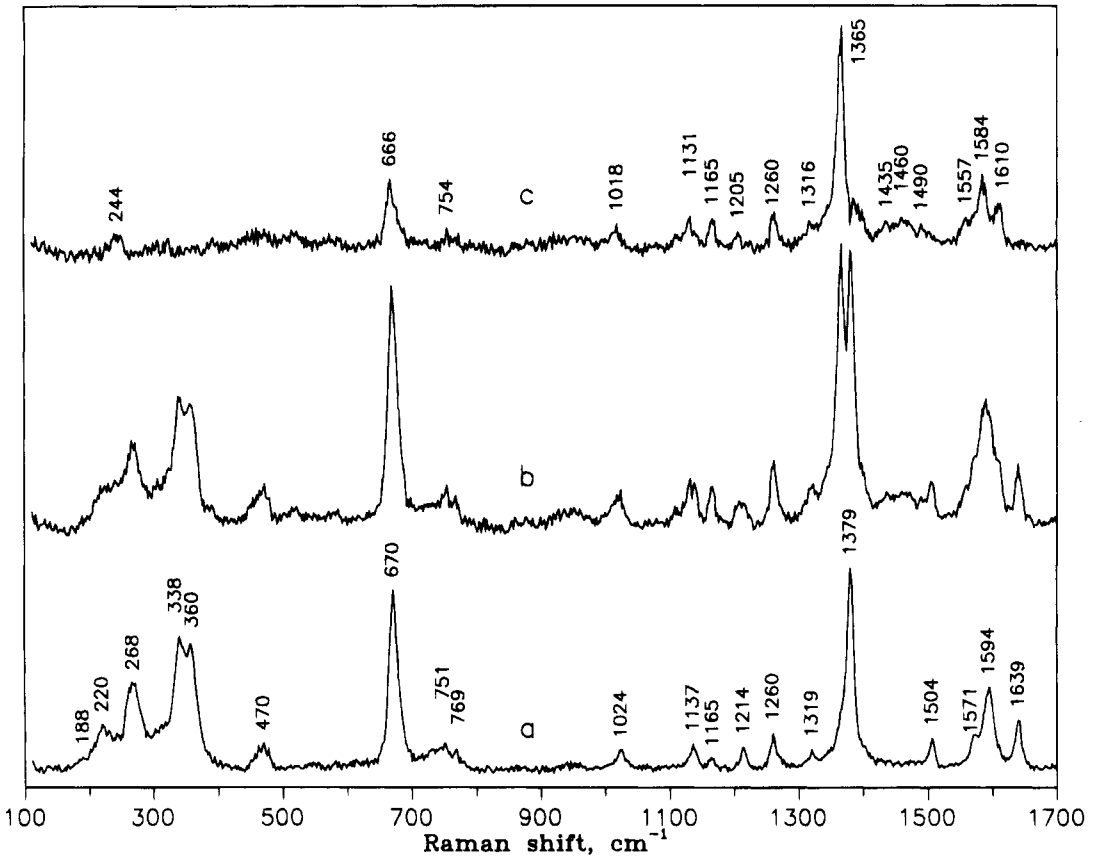

Figure 1. Transient RR spectra of CuOEP in THF recorded at 293 K with excitation at 400 nm. Spectrum a was obtained at low excitation power with a cylindrical lens, and spectrum b was obtained at high excitation power with a sharply focused spherical lens (for more details see Experimental Section). The difference spectrum (c) represents excited-state scattering (c = b − a). The subtraction procedure is described in the text. Solvent lines are eliminated in all spectra.

mainly by the solvent.[19] The CARS spectrometer geometry and techniques used were described in detail elsewhere.[20] Typical spectral resolution was 5 cm^{-1} for resonance Raman (RR) spectra and 0.5 cm^{-1} for RCARS spectra. Dye lasers and monochromator scanning, control of the laser beam intensities, and data acquisition and processing were provided by a PC computer and CAMAC standard equipment.

Picosecond absorption measurements were carried out on the spectrometer which has been described elsewhere.[21] It is based on a passively mode-locked Nd:$YAlO_3$ laser system that delivers a single pulse from the train. Second-harmonic pulses of a parametric light oscillator (PLO) with time duration 20 ps and energy up to 1 mJ were used for excitation. A broad-band continuum in the 400−650 nm range generated in a cell with D_2O was used as a probing beam in the case of difference spectra measurements. The kinetics of the absorption changes was probed by the radiation of another PLO tunable over the entire visible spectral region. The probing pulses energy was 10 μJ. The timing was performed, as usually in picosecond absorption techniques, by using an optical path delay between exciting and probing pulse, the delay line with a step-motor being managed by a computer.

The stationary absorption spectra were recorded on a Beckman UV 5270 spectrophotometer.

All the investigated metalloporphyrin samples were obtained from Dr. A. M. Shulga. Spectral grade solvents were employed: benzene, toluene, piperidine (pip), pyridine, THF, 1,4-dioxane, cyclohexanone, DMSO, and DMF. The concentrations of the Cu−porphyrins were adjusted for an absorption maximum of 0.5−2.0 in the Q-band region. During the recording of RR and RCARS spectra at room temperature, samples were contained in a rotating quartz cell with a 0.5 or 1 mm thickness to avoid heating effects and decomposition by successive nanosecond laser pulses. Picosecond absorption measurements were made in a standard spectrophotometric cell with a 1 mm thickness. The low-temperature measurements were carried out using an ad hoc evacuated quartz cell placed in a transparent Dewar vessel with liquid nitrogen. The absence of decomposition of the samples was checked by recording the stationary absorption and Raman spectra before and after the experiments.

Results and Discussion

A. Spectroscopic Evidence for the Specific Intermolecular Interaction between Cu−Porphyrins and O-Containing Solvents. *1. Transient RR and RCARS Spectra.* Figure 1 presents typical RR spectra of CuOEP in THF obtained with excitation at 400 nm in the Soret band. Spectrum a was recorded at low excitation power (I_{ex} = 10^5 W/cm^2), and spectrum b, at high excitation power (I_{ex} = 10^8 W/cm^2). From comparison of spectra a and b, the power-induced changes are clearly seen to be connected with the population of some transient electronic state in the intense nanosecond laser field. Spectrum c is a difference spectrum (c = b − a) corresponding to the Raman scattering from this transient state. The subtraction procedure for spectrum c was optimized to eliminate negative or positive peaks corresponding to the Raman scattering from the ground electronic state. Note that the procedure of solvent subtraction had been done before spectrum c was evaluated. Figure 2 shows RCARS spectra of CuOEP in THF obtained with 560 nm excitation of the Q_{0-0} absorption band and with a pumping intensity of $\approx 10^8$ W/cm^2. The "additional" transient peaks, arising with the increase of incident photon densities, are marked by "E" in Figure 2. Special investigations have shown that the ratio of amplitudes of any two "additional"

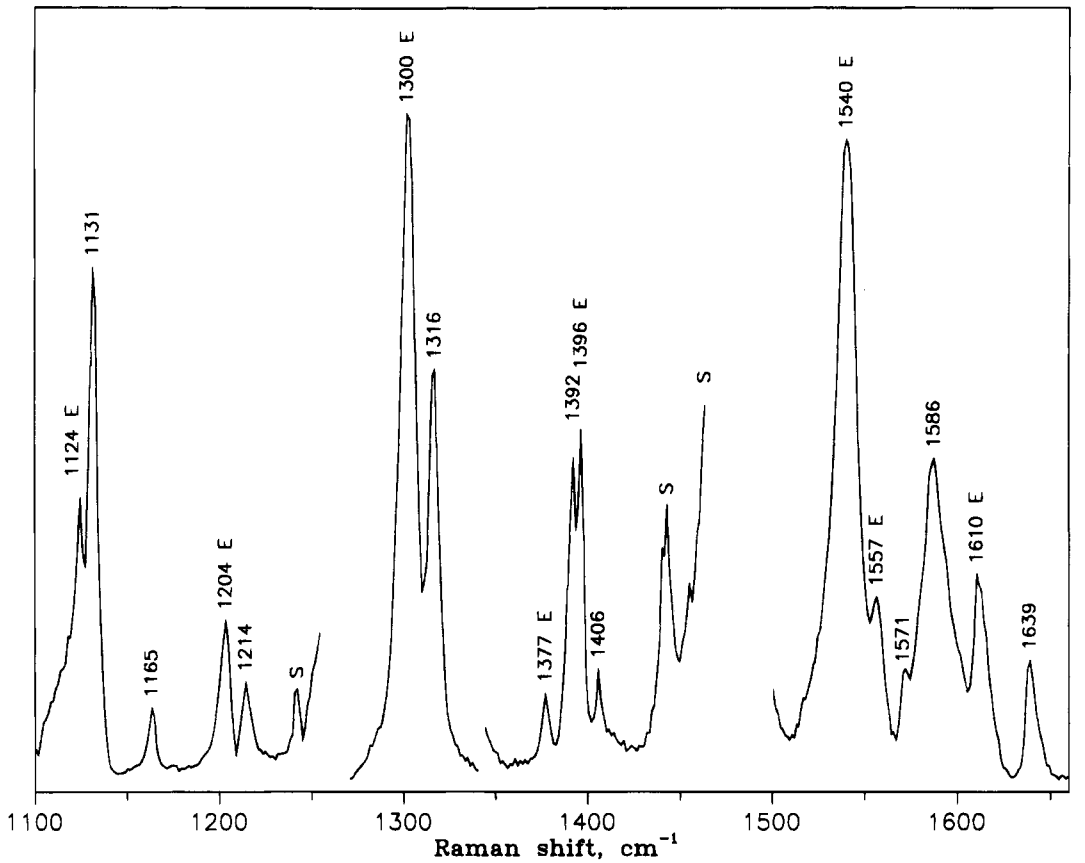

Figure 2. Background-free transient RCARS spectra of CuOEP in THF. Experimental conditions: $\lambda_1 = \lambda_3 = 560$ nm, $I_1 = 10^8$ W/cm^2. "S" indicates solvent lines. "E" corresponds to the Raman bands originated from the excited state.

lines in RCARS spectra does not depend upon excitation power. This fact proves that all "additional" lines originated from the same transient electronic state populated under high-power irradiation.

The appearance of new transient peaks was also observed for CuOEP dissolved in other O-containing solvents. Figure 3 shows RR spectra of CuOEP in a dioxane/toluene (1:1) mixture with Soret-band excitation, which exhibit in general the same features as with THF as a solvent.

The effect of photoinduced population of the excited state for CuOEP in various O-containing solvents was tested in RCARS spectra by examining the antisymmetric mode ν_{19} at 1586 cm^{-1} in the ground state; its excited state counterpart occurs at $\approx$1540 cm^{-1} (Figure 4). All the spectra in Figure 4 were recorded at the same value of excitation power of $\approx 10^8$ W/cm^2. It is seen from the spectra in Figures 2 and 4 that, in the case of CuOEP in THF and dioxane, it is possible to achieve more than 50% conversion of molecules into the transient excited state in the intensive nanosecond laser field. This conclusion can be made proceeding from the ratio of peak intensities I_{1540}/I_{1586} and on the assumption that the extinction coefficients in both states are nearly equal. For cyclohexanone (Figure 4c) and DMSO (Figure 4b), the effect of the population of the excited state can be reliably detected, but the share of the molecules in this state is small. And, finally, the transient peak near 1540 cm^{-1} is at the noise level of the RCARS spectrum of CuOEP in DMF (Figure 4a), so it is impossible to make any definite conclusion about the population of the transient electronic state in this case.

Power-induced changes were also observed in Raman spectra of copper complexes having various porphyrin ligands. Figure 5 presents RR spectra of copper *meso*-tetraphenylporphyrin (TPP) in a dioxane/toluene (1:1) mixture obtained with excitation at 436 nm. Figure 6 shows RR spectra of CuTPP in THF obtained with excitation to the maximum of the Soret band at 416 nm. In both cases, the effect of population of the transient electronic state under sufficiently high excitation intensity clearly manifests itself. Similar transformations of RR and RCARS spectra were also observed for CuTPP(*ortho*-F)$_4$, Cu–ethioporphyrin, and Cu–mesoporphyrin IX dimethyl ether in THF at high excitation power (not shown). So, the appearance of new transient peaks in Raman spectra recorded at high excitation power is found to be a rather common effect for Cu–porphyrins in O-containing solvents. It should be noted that for all the complexes investigated the photoinduced spectral changes were completely reversible and no decomposition products or appearance of new stationary spectral forms during the experiments were observed.

To a certain extent, RR and RCARS spectra related to the photoinduced transient electronic state (Figures 1–6) reveal similarity to the spectra originated from the ground state, except for the negative frequency shifts of several structure-sensitive marker lines. With this similarity of spectra in mind, RCARS amplitude-polarization measurements of Raman mode symmetries were performed according to the procedure described in refs 20 and 22. On the basis of these polarization measurements and proceeding from the closeness of the frequencies, the majority of the transient Raman bands are placed in unambiguous correspondence with their ground state counterparts. The results of such an assignment are given in Tables 1 and 2.

To elucidate the character of resonance enhancement of the scattering from the excited state in the visible region, we measured the excitation and probing profiles of nondegenerate RCARS. The results of this study for the most prominent antisymmetric mode ν_{19} for CuOEP in THF are presented in Figure 7. The technique implemented was described in detail elsewhere.[20] The nondegenerate RCARS process is defined as

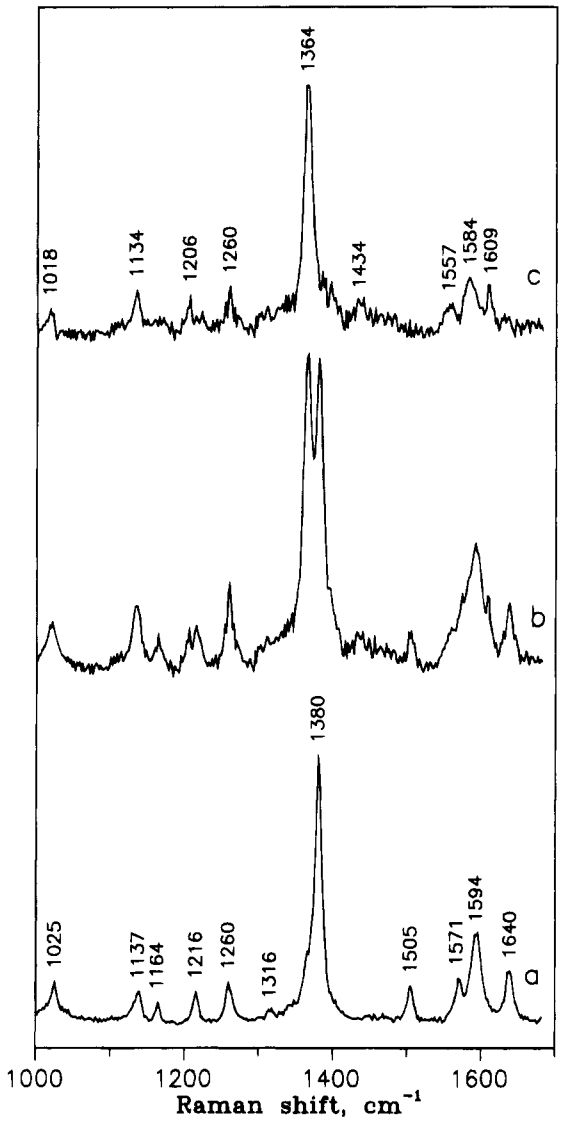

Figure 3. As in Figure 1, but of CuOEP in a dioxane/toluene (1:1) mixture.

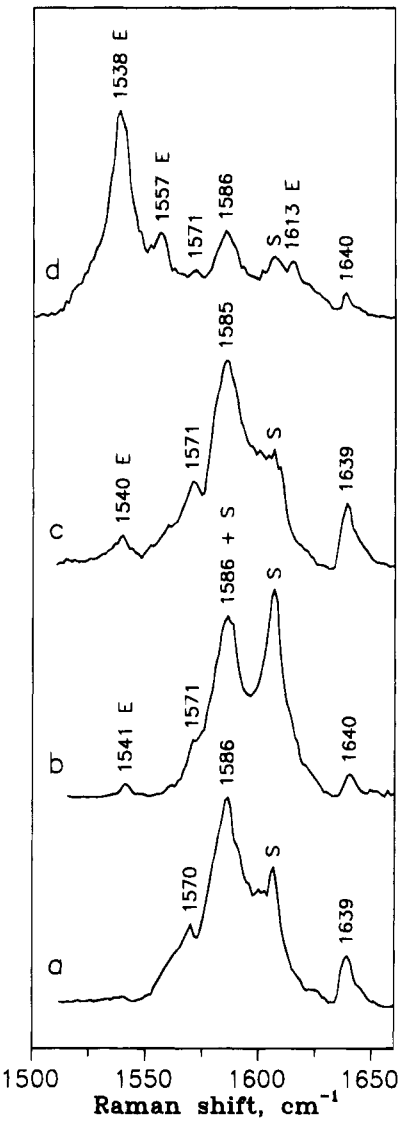

Figure 4. Background-free transient RCARS spectra of CuOEP in various oxygen-containing solvents: (a) DMF/toluene (1:1); (b) DMSO/toluene (1:1); (c) cyclohexanone/toluene (1:1); (d) dioxane/toluene (1:1). All spectra were recorded at the same experimental conditions: $\lambda_1 = \lambda_3 = 560$ nm, $I_1 = 10^8$ W/cm^2. "S" indicates solvent line. "E" corresponds to the excited state bands.

$\omega_{as} = \omega_3 + (\omega_1 - \omega_2)$, where ω_{as} is scattered frequency, ω_i ($i = 1-3$) represents incident waves, and the condition $\omega_1 - \omega_2 = \Omega$ is fulfilled (Ω represents frequency of the Raman mode being investigated). The scanning of the ω_1 frequency within the Q_{0-0} absorption band at fixed ω_{as} and $\omega_1 - \omega_2 = \Omega$ makes it possible to obtain the nondegenerate RCARS excitation profile $I_{as} = f(\omega_{0-0} - \omega_1)$ (Figure 7b). At the same time, the RCARS probing profile $I = f(\omega_{0-1} - \omega_{as})$ (Figure 7a) was recorded by fixing ω_1 and scanning ω_{as} within the Q_{0-1} absorption band. The power density of the radiation flux resonant to the Q_{0-0} absorption band was chosen in the 10^7-10^8 W/cm^2 range in order to obtain comparable intensities of the ground and excited Raman lines. The profiles presented in Figure 7 exhibit two maxima, one is located within the Q_{0-0} absorption band while another is shifted downward to the frequency of the vibrational mode investigated. It should be noted that the maxima of excitation profiles in the Q_{0-0}-band region were not measured precisely because of the experimental difficulties, since the wavelength 560 nm was the degenerate point and did not provide correct values of nondegenerate RCARS intensity. The main conclusion which may be derived from the measured profiles is that they generally mimic the vibronic absorption spectrum and reveal similarity for the modes from the ground and excited states except for the small red shift of the short-wavelength maximum corresponding to the excited-state mode. So, the excited-state counterpart of the mode ν_{19} reveals considerable enhancement within the Q-band region, behavior which is characteristic for the scattering not from the excited triplet (π,π^*) state but from the ground or excited (d,d) states of metalloporphyrins.

It should be noted that the effect of photoinduced population of a particular excited electronic state, detected in transient Raman spectra, is driven by the interaction of Cu−porphyrins with solvent molecules containing oxygen heteroatoms. Such a conclusion was made by us after additional investigations of Cu−porphyrins in both noncoordinating and N-containing solvents. And in both cases RR and RCARS spectra taken at high excitation power radically differ from those presented in Figures 1−6. Let us analyze at first the case of Cu−porphyrins in noncoordinating solvents.

As pointed out in the Introduction, the photoexcitation of Cu−porphyrins in the $S_0 \rightarrow S_n$ channel is followed by the ultrafast relaxation to the excited triplet state T_1, having a lifetime of 10−100 ns in noncoordinating solvents such as benzene or toluene. This lifetime is long enough to obtain a substantial population and record transient Raman spectra from the triplet (π,π^*) states with nanosecond laser pulses. The preliminary results of this investigation were published elsewhere.[26] A more

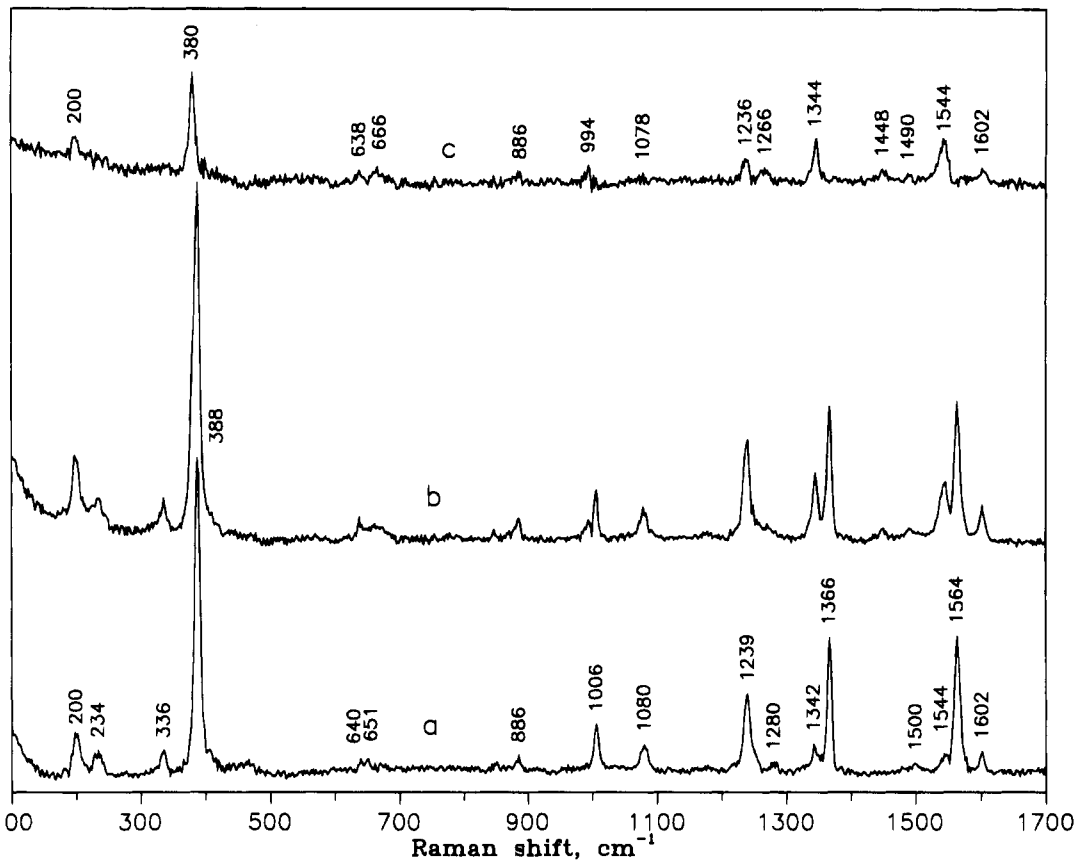

Figure 5. Transient RR spectra of CuTPP in a dioxane/toluene (1:1) mixture recorded using 436 nm excitation at low (a) and high (b) photon densities. The difference spectrum (c) represents excited-state scattering (c = b − a). Solvent lines are eliminated in all spectra.

detailed study on saturation and time-resolved RR spectra of the Cu−porphyrins' triplet (π,π^*) states is in progress now. Here it should only be noted that transient triplet Raman spectra differ greatly from the ground-state ones, breaking down the one-to-one analogy of the Raman-active vibrations of the ground- and excited-state species. So, assignment of the triplet Raman bands is a rather complicated problem because of the considerable broadening of lines and weakness of a number of the most prominent Raman bands of the porphyrin skeleton (for example ν_2 and ν_4 modes). These peculiarities of the triplet Raman spectra obtained by us are consistent with the results of triplet Raman studies on ZnTPP,[27,28] CuTPP,[29] ZnOEP,[30] and free-base porphyrins.[31] Therefore, we can reasonably infer that the appearance of new transient bands in Raman spectra for Cu−porphyrins in O-containing solvents under high excitation power cannot be ascribed to the triplet (π,π^*) excited-state species.

For Cu−porphyrins dissolved in N-containing solvents, the triplet T_1 state still remains the most long-lived excited state. But its lifetime is reduced by about 3 orders of magnitude due to the perturbing influence of the axial binding of a solvent molecule to central metal.[4,6−8] Very short decay times prevent a considerable population of the excited states with nanosecond laser pulses. Together with the weakness of scattering from the triplet subsystem of levels, this hinders reliable recording of transient Raman spectra from the excited triplet (π,π^*) state T_1. That is why all the recorded RR and RCARS spectra of Cu−porphyrins in N-containing solvents changed only slightly with variations of excitation power over the range 10^5-10^8 W/cm^2 and all the distinct lines in high-power spectra belonged to the ground electronic state.

2. Transient Absorption and Kinetics. The distinguishing feature of the relaxation process for Cu−porphyrins in a number of O-containing solvents is the double-exponential kinetics of spectral changes, and each of the two relaxation stages is characterized by its own transient absorption spectrum. Figure 8 presents difference spectra for CuOEP in THF obtained at short (a, 10 ps) and long (b, 300 ps) time delays following excitation to the maximum of the Q_{0-0} absorption band. Time evolution of the first spectrum was tested at 453 nm (Figure 9a): the transient absorption grows with the instrument-limited response and disappears by the exponential law with the relaxation time $\tau_1 = 140 \pm 10$ ps. Simultaneously with the first spectrum decay the second transient difference spectrum is formed (probing at 572 nm, Figure 9b), which then disappears by the exponential law with an average time constant of $\tau_2 = 360 \pm 40$ ps. Simultaneously with this process, the recovery of the ground-state bleaching occurs.

Spectra a and b in Figure 8 display different behavior in both the blue (450−500 nm) and green-yellow (520−590 nm) spectral regions. The first spectrum is marked by a broad structureless absorption in the blue region and bleaching in the strong ground-state Q_{0-0} band near 562 nm and in the weaker Q_{0-1} band at 525 nm. Such behavior is consistent with the triplet−triplet transient absorption of metalloporphyrins.[4,32] So, the first step of relaxation kinetics is inferred to represent the excited triplet state decay (it should be noted that the process of the conversion of initially excited singlet ^2S_n to the triplet $^2T_1$ is too fast to be observed, and the establishment of the tripdoublet−quartet equilibrium $^2T_1 \leftrightarrow {}^4T_1$ is characterized by very small absorption changes, so it was not taken into account). The measured triplet-state lifetime for CuOEP in THF ($\tau_1 = 140$ ps) is much shorter than the usual value for CuOEP in noncoordinating solvents ($\tau_1 = 120$ ns in toluene) and is comparable to the triplet-state lifetime for Cu−porphyrins in N-containing solvents.[4,6−8]

The transient difference spectrum in Figure 8b related to the second stage of the relaxation kinetics is characterized by derivative-like absorption changes in the green-yellow spectral

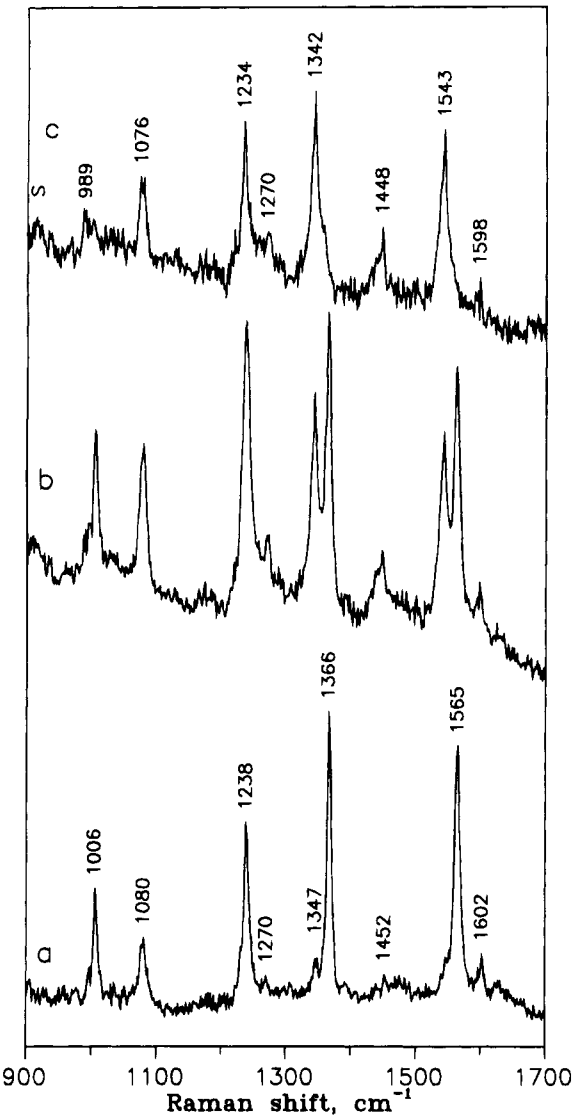

Figure 6. As in Figure 5, but of CuTPP in THF using 416 nm excitation.

region. Transient absorption appears immediately to the red of the bleaching of the ground-state Soret and Q bands while there are no distinct absorption changes in the blue region. Thus, it can be stated that the second transient species has an absorption spectrum similar, in general terms, to that of the ground-state one of CuOEP, but with a red shift in the absorption band maxima. Note that such behavior is characteristic for transient absorption spectra from the excited (d,d) (namely $^3B_{1g}$) state of Ni–porphyrins.[4,32]

Similar double-exponential relaxation kinetics was also observed for CuOEP in dioxane and cyclohexanone/toluene as well as for CuTPP in THF, dioxane/toluene, and cyclohexanone/toluene. For example, Figure 10 presents the kinetic data for absorption changes for CuTPP in THF obtained with probing at 499 and 446 nm.

At the same time for Cu–porphyrins in DMF and DMSO, the decay of the transient absorption was found to be single-exponential, the effect being similar to the one observed earlier for Cu–porphyrins in N-containing solvents.[4,6–8] We undertook careful transient absorption measurements for CuOEP in DMF, DMSO, and pyridine at various delay times in order to find signs of the second transient species, populated in the course of excitation relaxation. However, nothing was found: in all cases we measured only single-exponential decay of absorbance changes and simultaneous recovery of the ground-state bleaching with the time constant of ≈100–200 ps. Note that the transient difference absorption spectra of CuOEP in the above solvents (not shown) were found to be very similar to the spectrum of the first transient species for CuOEP in THF (Figure 8a), representing triplet–triplet transient absorption.

The kinetic data are summarized in Table 3.

TABLE 1: Observed Raman Frequencies (cm^{-1}) of the Prominent Bands in RR and RCARS Spectra from the Ground and Excited States for CuOEP

designation[a]			ground state				exc state	
mode	sym	contribution[b]	THF[c]	diox[c]	pip[d]	77 K[e]	THF[c]	diox[c]
ν_{10}	B_{1g}	$\nu(C_aC_m)$	1639	1640	1637	1640	1610	1613
ν_2	A_{1g}	$\nu(C_bC_b)$	1594	1594	1590	1597	1584	1584
ν_{19}	A_{2g}	$\nu(C_aC_m)$	1586	1586			1540	1538
ν_{11}	B_{1g}	$\nu(C_bC_b)$	1571	1571	1567	1573	1557	1557
ν_3	A_{1g}	$\nu(C_aC_m) + \nu(C_bC_b)$	1504	1505	1502	1504	1490	
Et	A_1	CH_2 scissors					1460	
Et	E	CH_2 scissors					1435	1434
ν_{29}	B_{2g}	$\nu(C_aC_b)$	1406				1396	
ν_{20}	A_{2g}	$\nu(C_aN) + \nu(C_aC_b)$	1392				1377	
ν_4	A_{1g}	$\nu(C_aN) + \nu(C_aC_b)$	1379	1380	1378	1382	1365	1364
Et	A_1	CH_2 wagging	1319	1316		1322	1316	
ν_{21}	A_{2g}	$\nu(C_aN) + \delta(C_aC_mH)$	1316	1316			1300	1299
Et	A_1	CH_2 twisting	1260	1260	1259	1267	1260	1260
ν_{13}	B_{1g}	$\delta(C_mH) + \nu(C_aC_b)$	1214	1216	1214	1220	1205	1206
ν_{30}	B_{2g}	$\nu(C_aN) + \nu(C_bC_1)$	1165	1164	1164	1165	1165	
ν_5	A_{1g}	$\nu(C_aC_b) + \nu(C_bC_1)$	1137	1137	1137	1140	1131	1134
ν_{22}	A_{2g}	$\nu(C_aN) + \delta(C_aC_mH)$	1131				1124	
Et	A_1	$\nu(C_1C_2)$	1024	1025	1021	1025	1018	1018
Et	A_1	CH_2 rocking	769		767	769	754[f]	
ν_{15}	B_{1g}	pyrrole breathing	751		749	749		
ν_7	A_{1g}	core breathing	670	672	669	671	666	665
Et	B_{1u}	$\delta(C_bC_1C_2)$	470		464	484[g]		
ν_8(B)	A_{1g}	$\delta(C_bC_1)$	360		357	359		
ν_8(A)	A_{1g}	$\delta(C_bC_1)$	338		338	344		
ν_9	A_{1g}	$\delta(C_bC_1)$	268		269	280	244[f]	
oop	E_g	$\gamma(C_aC_m)$	220		221			
ν_{18}	B_{1g}	ν(CuN)	188		184	150[f]		

[a] Mode designation according to refs 23 and 24. [b] Main internal coordinate contribution to the mode, as determined in refs 23–25. [c] λ_{exc} = 400 nm for RR and 560 nm for RCARS spectra in THF and 1,4-dioxane/toluene (1:1) (diox) solvents. [d] λ_{exc} = 402 nm for spectrum in piperidine (pip) solvent. [e] Low temperature (T = 77 K) measurements in a THF/diethyl ether (1:1) mixture with λ_{exc} = 405 nm (oop modes observed with excitation at 400 nm are not presented). [f] Correct assignment was not made. [g] The broad band at 470 cm^{-1} (293 K) is split at 77 K into three bands at 438, 466, and 484 cm^{-1}.

TABLE 2: Observed Raman Frequencies (cm^{-1}) of the Prominent Bands in Spectra from the Ground and Excited States for CuTPP

designation[a]			ground state				exc state	
mode	sym	contribution[a]	diox[b]	THF[c]	benz[d]	pip[d]	diox[b]	THF[c]
ϕ_4	A_{1g}	$\nu(CC)_{Ph}$	1602	1602	1600	1600	1602	1598
ν_2	A_{1g}	$\nu(C_aC_m) + \nu(C_bC_b)$	1564	1565	1563	1559	1544	1543
ν_{11}	B_{1g}	$\nu(C_bC_b)$	1500			1496	1490	
ϕ_5	A_{1g}	$\delta(CCH)_{Ph} + \nu(CC)_{Ph}$						
ν_{28}	B_{2g}	$\nu(C_aC_m) + \delta(CCH)_{Ph}$			1474			
ν_3	A_{1g}	$\nu(C_bC_b) + \nu(C_aC_m)$		1452	1458		1448	1448
ν_4	A_{1g}	$\nu(C_aC_b) + \nu(C_aN)$	1366	1366	1364	1361	1344	1342
ν_{27}	B_{2g}	$\nu(C_mPh) + \nu(C_aN)$	1280	1270	sh[e]	sh	1266	1270
ν_1	A_{1g}	$\delta(C_mPh)$	1239	1238	1237	1236	1236	1234
ν_9	A_{1g}	$\delta(C_bH)$	1080	1080	1079	1077	1078	1076
ν_6	A_{1g}	$\nu(C_aC_b) + \nu(C_aN)$	1006	1006	1004	1004	994	989
ϕ_8	A_{1g}	$\delta(CCC)_{Ph}$					sh	sh
ν_7	A_{1g}	$\delta(CC)_{Ph} + \nu(CC)_{Ph}$	886	886	886	886	886	
$2\nu_8$	A_{1g}			779	778	779		
γ_{20}	E_g	oop, pyrrole fold	651	673			666	
ϕ_9	A_{1g}	$\delta(CCC)_{Ph}$	640	641	639	639	638	
ν_8	A_{1g}	ν(CuN)+$\delta(C_aC_mCa)$	388	392	389	395	380	
γ_2	A_{1u}	oop, pyrrole swivel	336	340	336	341		
ν_{13}	B_{1g}	$\gamma(C_mC_{Ph}) + \tau(CC)_{Ph}$	234	233				
ϕ_{10}	A_{1g}	$\delta(CCC)_{Ph} + \nu(C_mC_{Ph})$	200	202	200	207	200	

[a] Modes designation and main internal coordinate contribution to the mode according to ref 24a. [b] λ_{exc} = 436 nm. [c] λ_{exc} = 416 nm. [d] λ_{exc} = 402 nm. [e] sh = shoulder.

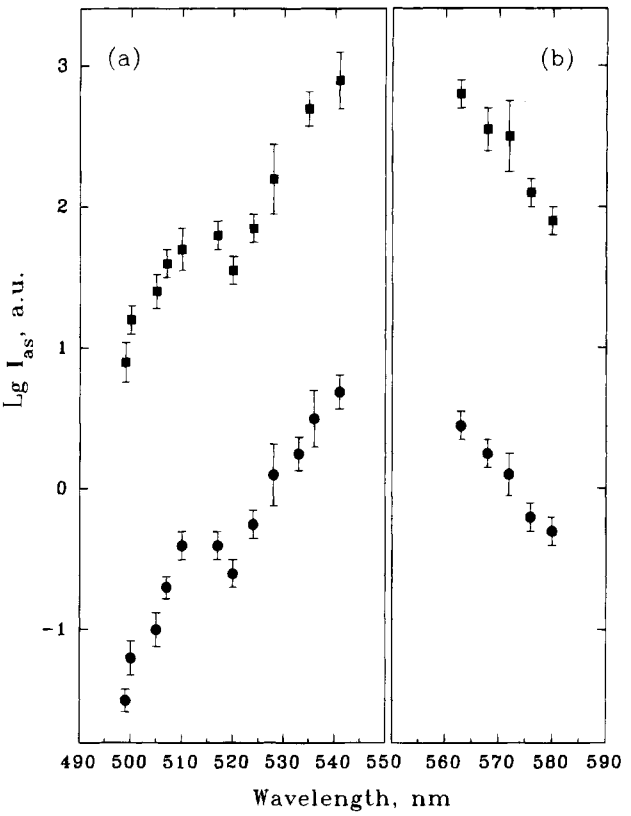

Figure 7. Nondegenerate RCARS probing (a) and excitation (b) profiles in the Q-band region for mode ν_{19} in the ground (●) and excited (■) states for CuOEP in THF. The experimental conditions were as follows: (a) $\lambda_1 = 560$ nm, $I_1 = 10^8$ W/cm^2, $I_1 \gg I_2$, I_3, polarization configuration of incident waves, $\mathbf{e}_3 \wedge \mathbf{e}_1 = 45°$, $\mathbf{e}_2 \wedge \mathbf{e}_1 = 90°$, $\mathbf{e}_{as} \wedge \mathbf{e}_1 = 135°$; (b) $\lambda_3 = 560$ nm, $I_3 = 10^8$ W/cm^2, $I_3 \gg I_1$, I_2, $\mathbf{e}_3 \wedge \mathbf{e}_1 = -45°$, $\mathbf{e}_2 \wedge \mathbf{e}_1 = 45°$, $\mathbf{e}_{as} \wedge \mathbf{e}_1 = 90°$. For more details see text and ref 20.

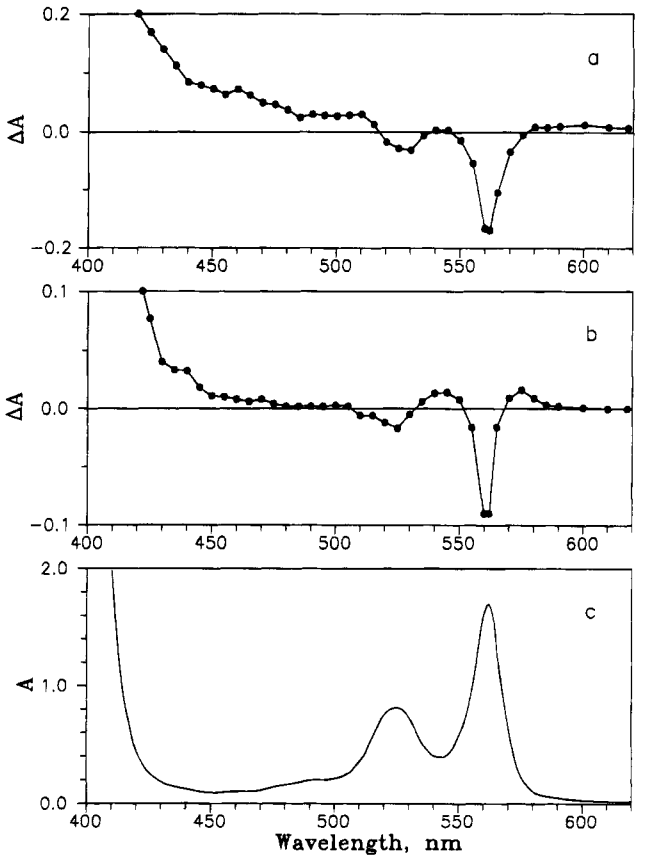

Figure 8. Transient absorption spectra for CuOEP in THF obtained at short (a, $\tau = 10$ ps) and long (b, $\tau = 300$ ps) time delays following excitation with 562 nm flashes. Spectrum c displays ground-state absorption.

B. Nature of the Exciplex. *1. General Consideration.* On the basis of the results obtained, Cu−porphyrins are inferred to interact specifically with the molecules of O-containing solvents. This interaction manifests itself in both transient Raman spectra (the appearance of new transient peaks at high excitation intensity) and picosecond difference absorption measurements (the presence of double-exponential kinetics of absorption changes and the decrease of the triplet (π,π^*) excited-state lifetime). What is the nature of this interaction? Proceeding from the well-known ability of Cu−porphyrins to bind a molecule of nitrogen bases as an axial ligand, it is tempting to assume that a similar process is possible with participation of the organic molecules containing oxygen heteroatom(s).

Let us first analyze the possibility of coordination of O-containing molecules to Cu−porphyrins in the ground electronic state. A comprehensive study of the stationary absorption spectra of CuOEP in THF, toluene (Figures 11a and 12a), and chloroform (not shown) proves that these spectra are very similar: for all solvents used the absorption maxima are at the same wavelengths with the accuracy ±1 nm. Since the last two solvent molecules do not contain heteroatoms and cannot be coordinated to the metal, CuOEP in the ground electronic state in THF at room temperature has to be considered exclusively as a four-coordinate species. At the same time, the observed dramatic decrease of the triplet-state lifetime for CuOEP in THF as compared to the case of noncoordinating solvents (Table 3) is indicative of the quenching influence of solvent molecules. So, it is reasonable to assume that the photoexcitation of the porphyrin molecule increases its affinity for ligation by O-containing molecules, and an excited bimolecular complex is formed (so-called exciplex [(CuP)*−L], where L represents an axially ligated THF molecule). Since the Cu−porphyrin, after $S_0 \rightarrow S_n$ photoexcitation, relaxes extremely rapidly to the triplet state T_1,[4-9] this exciplex is inferred to form when a solvent molecule is ligated by a four-coordinate porphyrin species in the excited triplet state.

The characterization of the transient excited-state species, which serves as the "bottleneck" state for deactivation of the exciplex and is manifested by the new transient peaks in Raman spectra at high excitation power, is essential for a complete understanding of the processes under investigation. According to absorption kinetic measurements, this transient species may relate either (i) to the exciplex being in the excited triplet (π,π^*) state [(CuP)*$_{T_1}$−L] or (ii) to the product of the further electronic energy relaxation inside exciplex. It is known that the ligated Cu−porphyrin species has spectra (both Raman and absorption) similar to those of the corresponding noncomplexed species.[7,14] So, if the first assumption is valid, transient Raman spectra as well as absorption difference spectra should be similar to those originated from the triplet state of nonligated Cu−porphyrins.[4,26,29] But, according to the above discussion, this is not the case. Moreover, the nondegenerate RCARS profile measurements also prove the "nontriplet" character of the transient Raman peaks appearing at high excitation power. Therefore, we concluded that the exciplex "bottleneck" transient state is populated in the course of the triplet (π,π^*) excitation decay. Now we consider in more detail the possible decay pathways.

The axial binding of a σ-donor O-containing solvent molecule to the central copper ion should cause the perturbation of the porphyrin molecular orbitals with subsequent shifts of the excited CT and (d,d) states to lower energies. Let us recall here that a similar process was observed for N-containing solvents[4,6-8,14] and was theoretically calculated for water as an axial ligand.[7,14] According to Kim et al.,[7] in the process of chemical bond formation between solvent molecule and met-

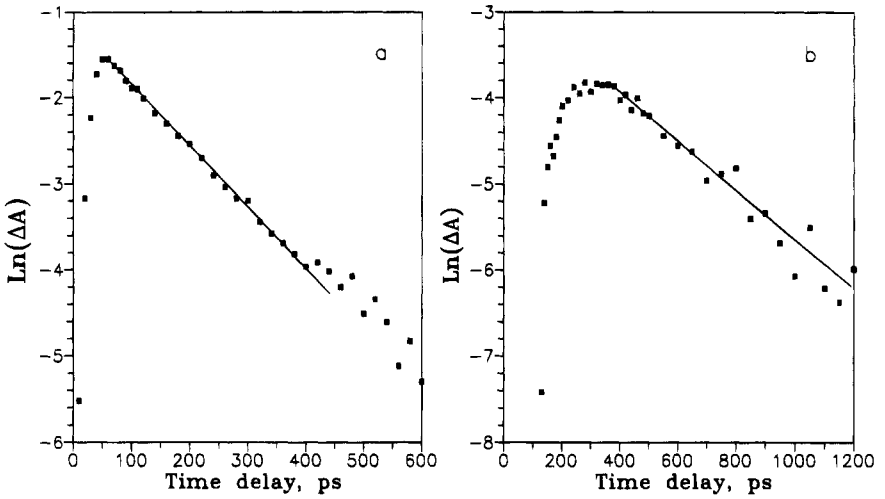

Figure 9. Kinetics of absorption changes for CuOEP in THF with excitation at 560 nm and probing at 453 nm (a, short-decay component) and 572 nm (b, long-decay component). Solid curves represent best-fit lines through the experimental data points: $\tau_1 = 140$ ps, $\tau_2 = 360$ ps. Note the ordinate is a log scale.

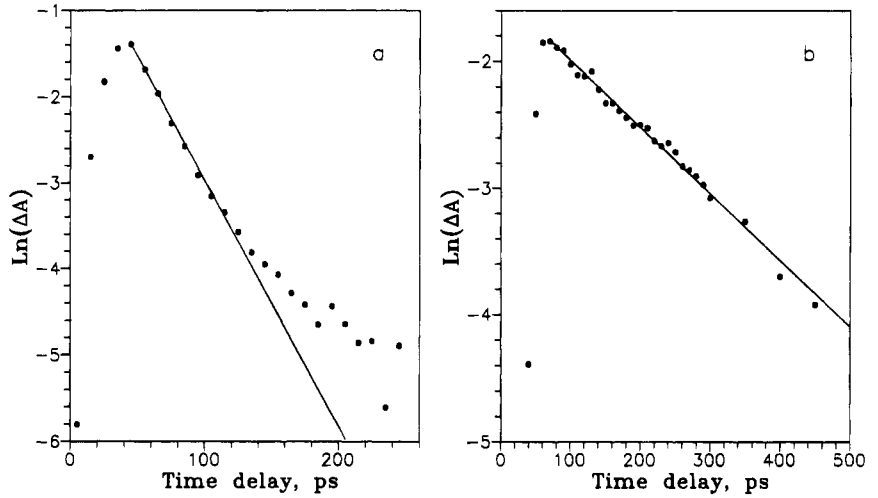

Figure 10. Kinetics of absorption changes for CuTPP in THF with excitation at 544 nm and probing at 499 nm (a, short-decay component) and 446 nm (b, long-decay component). Solid curves represent best-fit lines through the experimental data points: $\tau_1 = 35$ ps, $\tau_2 = 190$ ps. Note the ordinate is a log scale.

TABLE 3: Summary of Kinetic Data for Copper Porphyrins

compound	solvent	τ_1, ps	τ_2, ps
CuOEP	toluene	120×10^3	
	pyridine	80 ± 10	
	tetrahydrofuran	140 ± 10	360 ± 40
	tetrahydrofuran/diethyl ether (1:1)	280 ± 40	360 ± 40
	1,4-dioxane	65 ± 10	345 ± 40
	cyclohexanone/toluene (1:1)	450 ± 150	?[a]
	dimethyl sulfoxide/toluene (1:1)	215 ± 20	
	dimethyl formamide/toluene (1:1)	175 ± 20	
CuTPP	toluene	35×10^3	
	pyridine	45 ± 15	
	tetrahydrofuran	35 ± 10	190 ± 10
	1,4-dioxane/toluene (1:1)	100 ± 10	395 ± 40
	cyclohexanone/toluene (1:1)	400 ± 40	560 ± 40
	dimethyl sulfoxide/toluene (1:1)	200 ± 20	
	dimethyl formamide/toluene (1:1)	130 ± 10	

[a] The two kinetics have not been correctly distinguished.

alloporphyrin, an intersection of the lowered CT and/or (d,d) terms with the $^{2,4}T_1$ levels has to occur. As a result, rapid triplet excitation relaxation can proceed via one of these lowered excited states of the resulting five-coordinate complex on a picosecond time scale. In the framework of this model, the lifetime τ_1 (Table 3), characterizing the decay kinetics of the triplet state of a nonligated Cu−porphyrin, is the rate of diffusion-controlled mutual movement, mainly reorientational, of the triplet-excited Cu−porphyrin and surrounding O-containing solvent molecules L. This process is followed by the formation of exciplex species $[(CuP)^*_{T_1}-L]$ (the ligated species is apparently indistinguishable from $(CuP)^*_{T_1}$) and its instantaneous transition to a more low-lying excited state of (d,d) or CT nature. Accordingly, the second observed transient absorption spectrum represents either the low-lying CT or (d,d) excited state of the exciplex, with the lifetime τ_2 reflecting the excitation relaxation to the ground state and disruption of the exciplex into initial components.

The diffusion-controlled mechanism of Cu−porphyrin triplet-state quenching is confirmed by the observation that the lifetime τ_1 increases as the ligand concentration is reduced. Indeed, the reduction of THF concentration by half by dilution in diethyl ether (1:1) leads to doubling of the decay time τ_1 for CuOEP. Proceeding from the measured lifetime of the triplet state for CuOEP in THF ($\tau_1 = 140$ ps) and the known concentration of neat THF ([L] = 12.35 M), we calculate the second-order rate constant of the CuOEP triplet-state quenching by THF: $k = \tau_1[L]^{-1} = 5.8 \times 10^8$ M^{-1} s^{-1}.

The correspondence of the additional Raman peaks arising in transient RR and RCARS spectra at high excitation power to the second transient absorption species (τ_2) but not to the first one (τ_1) is confirmed by several reasons. First, this second

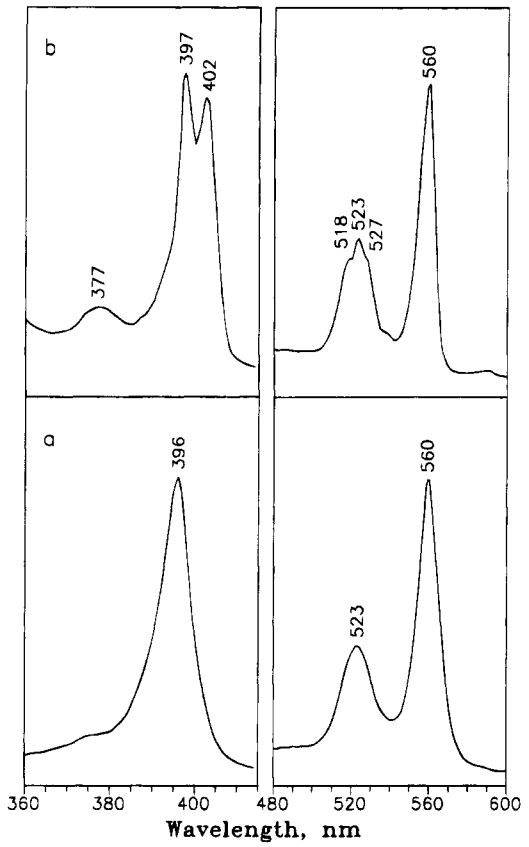

Figure 11. Absorption spectra of CuOEP in a THF/diethyl ether (1:1) mixture at 293 K (a) and 77 K (b).

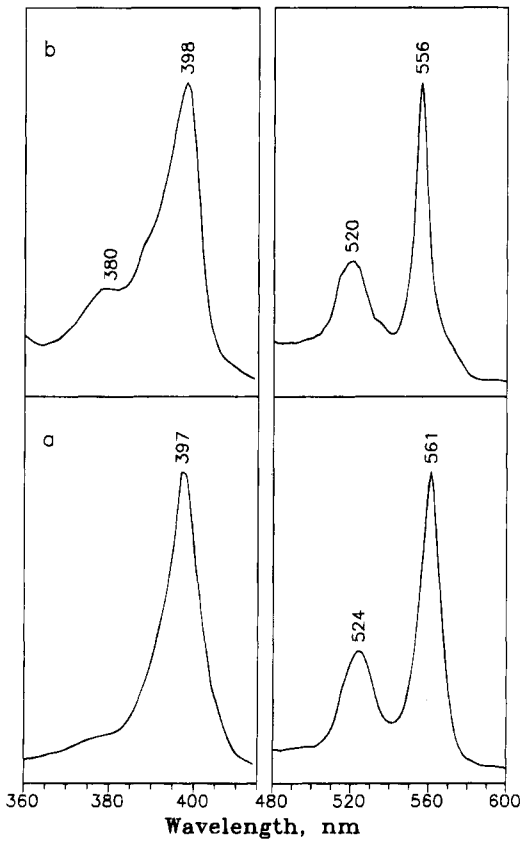

Figure 12. As in Figure 11, but in a toluene/diethyl ether (1:1) mixture.

transient species is the most long-lived one. Therefore, as the power increases, it is the first to be populated in a nanosecond laser field, giving new features in transient Raman spectra. Second, Raman excitation profiles for additional lines generally mimic vibronic absorption spectra, with maxima being slightly shifted to the red of the ground-state absorption band maxima. And such behavior is also characteristic of the absorption related to the second spectral form in relaxation kinetics. What is the nature of this transient species? Analysis of the whole set of experimental data permits supposing that this species is assignable to the excited (d,d) state of the five-coordinate Cu–porphyrin, which involves the net promotion of one of the two copper electrons in the d_{z^2} orbital into the half-filled $d_{x^2-y^2}$ orbital. Let us consider the experimental facts supporting this assumption.

First of all, vibrational analysis of transient Raman spectra proves this assignment. Indeed, structure-sensitive modes of the porphyrin skeleton in the high-frequency region in the excited state exhibit remarkable downshifts with respect to their ground-state counterparts. The maximum downshift value is 45 cm^{-1} for the mode ν_{19} for CuOEP in THF. A similar behavior is characteristic for the scattering from the excited (d,d) state of metalloporphyrins, namely, from the $^3B_{1g}$ state of Ni-porphyrins, which have been thoroughly studied in the last years.[16a,20,33–36]

Second, in the excited (d,d) state the porphyrin ring is essentially in its ground-state π-electronic configuration. Therefore, the absorption spectrum of this excited state (as well as the excitation profiles of Raman bands), corresponding to the (π,π^*) transition, should be basically the same as the ground-state one, but having slightly shifted bands as a result of the perturbation due to (d,d) excitation. This conclusion is supported by picosecond absorption studies of the excited (d_{z^2},$d_{x^2-y^2}$) state of the four-coordinate Ni-porphyrins[4,32,37,38] and the (d_π,d_{z^2}) state of cobalt complexes CoOEP(CN),[39] where derivative-like absorption difference spectra have been obtained in the Q-band region with strong transient absorption in the red to the Soret-band bleaching. The measurement of RCARS excitation profiles of Raman bands originated from the $^3B_{1g}$ state of NiOEP in THF also proves this statement.[20] Since for Cu–porphyrins in O-containing solvents the RCARS excitation/probing profiles (Figure 7) and corresponding transient absorption spectrum (Figure 8b) reveal similar behavior, it is indicative of the presence of d-electronic excitation.

As mentioned above, the other excited state, namely the (π,d) CT state, arising from the transfering of electronic density from the highest occupied molecular orbital (a_{1u} or a_{2u}) to the half-filled metal orbital $d_{x^2-y^2}$, could be proposed as a candidate to explain the above phenomena. To a first approximation, this CT state should exhibit spectral peculiarities similar to those of the π cation radicals of copper porphyrins ($CuP^{\bullet+}$). The Raman spectra of a_{1u} radicals of OEP complexes have been studied in detail.[40,41] It has been found that the structure-sensitive modes of $CuOEP^{\bullet+}$ exhibit both frequency downshifts (ν_3, ν_4, ν_{10}) and upshifts (ν_2, ν_{11}), with the greatest upshift being 37 cm^{-1} for the ν_{11} mode. Such behavior contradicts the changes in the transient Raman spectra of CuOEP in O-containing solvents obtained at high excitation power (Figures 1–4, Table 1). Raman studies of the $CuTPP^{\bullet+}$ a_{2u} π cation radical[41b,42] have also revealed different values of frequency shifts with respect to the mode shifts in Raman spectra originated from the excited state (Figures 5 and 6, Table 2), although the directions of the shifts are the same.

It should also be noted that the absorption spectrum of $CuTPP^{\bullet+}$ displays broad structureless absorption to the blue of the Soret-band region.[41b] Transient absorption spectra of the (d,π^*) CT excited states of ruthenium–porphyrin complexes[32,43] are marked by similar strong broad absorption but with the red shift in the Soret band. Besides, the excited CT state of a ring-to-metal origin is reliably distinguished by a prominent absorp-

tion band at ≈660 nm,[32,43] as $\Delta A = 0$ in this region for transient absorption originated from the ground and excited (d,d) states of metalloporphyrins. Our kinetic measurements of both CuOEP and CuTPP in THF and dioxane with probing at wavelengths > 600 nm revealed single-exponential kinetics of absorbance changes, related to the transient absorption from the triplet (π,π^*) states. No signs of the second, more long-lived transient species were found, that being the indication of the absence of absorption from this species within the 600−700 nm spectral region.

Proceeding from all these facts, we conclude that the observed second, more long-lived transient species, populated in the course of relaxation of the triplet (π,π^*) electronic excitation for Cu−porphyrins in a number of O-containing solvents, is assignable to the excited (d,d) state. The assignment of this transient species to the CT state involving molecular a_{1u} or a_{2u} orbitals of the porphyrin macrocycle is less probable.

2. Study of Cu−Porphyrin Complexation in the Ground Electronic State. Another possibility exists: an assignment is possible for the observed second, more long-lived transient species to the ground electronic state of the nonequilibrium complex [CuP−L] formed in the course of excitation relaxation. Indeed, this complex is thermodynamically unstable at room temperature and, once formed, must quickly disrupt into initial components. In this case, the time constant τ_2 reflects the disruption kinetics. Several arguments support the possibility of this explanation. First, binding of axial σ-donor ligands to Cu- and Ni-porphyrins in the ground electronic state results in the red shift of the absorption band maxima without a significant change in the general character of the spectra.[2,7] Moreover, the expansion of the porphyrin core that accompanies axial ligation results in substantial low-frequency shifts of structure-sensitive vibrational modes. For example, Raman studies of Ni-porphyrins in strong organic N-containing bases[44,45] have shown that the formation of a six-coordinate high-spin complex leads to a decrease in the marker line frequencies up to 50 cm^{-1}. These facts are in reasonable accord with the results obtained for Cu−porphyrins in O-containing solvents. Therefore, in order to support or reject the above alternative explanation, we ran additional studies of Cu−porphyrin complexation in the ground electronic state.

The lowering of the temperature of a solution containing a metalloporphyrin M and a potential axial ligand L leads to the shift of equilibrium constant toward the complex ML formation because of the diminishing of the thermal energy excess. Therefore, we have conducted low-temperature investigations of CuOEP in a THF/diethyl ether (1:1) mixture which forms a good glass at liquid nitrogen temperature. The absorption spectrum of this sample at 77 K displays characteristic splitting of the Soret band (Figure 11b, left panel), indicating coordination with THF. The Soret band at 397 nm is typical of CuOEP in noncoordinating solvents (Figure 12, left panels) while the red-shifted band with a maximum at ≈402 nm is assignable to the complexed species. This assignment is confirmed by a luminescence excitation study where only one 397 nm band was observed. The approximately equal intensities of the Soret bands (Figure 11b, left panel) point to the fact that ≈50% of CuOEP molecules have an axial ligand bound to the metal.

In the Q-band region, a solution freezing causes more complicated changes in the absorption spectrum: besides the maximum at 523 nm, which is characteristic of the room-temperature spectrum, shoulders at 518 and 527 nm appear, while the maximum of the Q_{0-0} band at 560 nm remains practically unaltered (Figure 11b, right panel). Such a complicated behavior of the absorption spectrum in the visible region may be accounted for by the combined effects of the two opposite factors. On the one hand, the complex formation results in the red shift of the absorption bands. On the other hand, it is known that the lowering of the temperature of a solution containing metalloporphyrin in noncoordinating solvent causes a blue shift of the Q absorption bands. For example, in the spectrum of CuOEP in a toluene/diethyl ether (1:1) mixture, the maxima of the Q bands shift from 524 and 561 nm at room temperature (Figure 12a, right panel) to, respectively, 520 and 556 nm at 77 K (Figure 12b, right panel). Note the position of the Soret-band maximum in this complex remains practically unaltered with no evidence of splitting, indicating the absence of complexation (Figure 12b, left panel). So, we believe that for CuOEP in THF at 77 K the overall red shift in the Q bands due to complexation is partially compensated by the blue shift associated with the decrease in the solution temperature. At the same time, the presence of some noncomplexed CuOEP molecules leads to the appearance in the spectrum of spectral features blue-shifted with respect to the room-temperature absorption band maxima.

Figure 13 presents low-temperature Raman spectra of CuOEP obtained with excitation at three different wavelengths within the Soret-band region. Special efforts were undertaken to minimize the effects associated with the population of the excited states: the sample illumination intensity was reduced to 10^5 W/cm^2. The only one small photoinduced transient line at ≈1365 cm^{-1} originated from the excited state is distinct in the low-temperature spectra. Further lowering of the excitation power leads to considerably worse quality of Raman spectra due to a decrease in the signal to noise ratio. So, it is impossible to eliminate completely the excited-state population under nanosecond pulsed illumination, presumably because of the longer lifetime of a photoinduced species at 77 K.

Let us analyze the changes in marker Raman band frequencies due to axial ligation of CuOEP in the ground electronic state. The characteristic feature of the low-temperature spectra of both noncomplexed and complexed species, effectively excited at 400 nm (Figure 13a) and at 405 nm (Figure 13c), respectively, is the rather small high-frequency shifts of Raman bands with respect to their room-temperature counterparts originated from the noncomplexed species (Figure 1, Table 1). Indeed, the ethyl substituent twisting mode exhibit the greatest shift (1260 → 1267 cm^{-1}) while the core-size marker lines of the porphyrin skeleton are shifted by no more than 3 cm^{-1}. The small high-frequency shifts of the modes ν_{10}, ν_2, and ν_{11} are indicative of a weak contraction of the porphyrin core and can be attributed to the environmental influence in the solute. Such behavior of the Raman marker bands reveals a negligible perturbation of the porphyrin structure by a ligand molecule attached to the copper ion and does not correlate with the photoinduced changes in the transient RR and RCARS spectra of CuOEP obtained at high excitation power at room temperature.

We have also studied the ground-state complexes of Cu−porphyrins with N-containing molecules at room temperature. Figure 14 shows the Raman spectrum of CuOEP in piperidine; the percentage of the complexed molecules in this solvent is known to be 50−70%.[7] Figure 15 presents Raman spectra of CuTPP in both coordinating piperidine, for which >90% of the CuTPP appears to be complexed,[7] and noncoordinating benzene. For complexed forms of both Cu−porphyrins, Raman lines exhibit shifts by no more than 10 cm^{-1} with respect to their counterparts of noncomplexed species (see also Tables 1 and 2). Note this result is consistent with an earlier obtained Raman spectra of Cu−porphyrins in various coordinating solvents.[14]

Thus, in the course of these spectroscopic determinations, we found that binding of both oxygen- and nitrogen-containing molecules as axial ligands by Cu−porphyrins in the *ground*

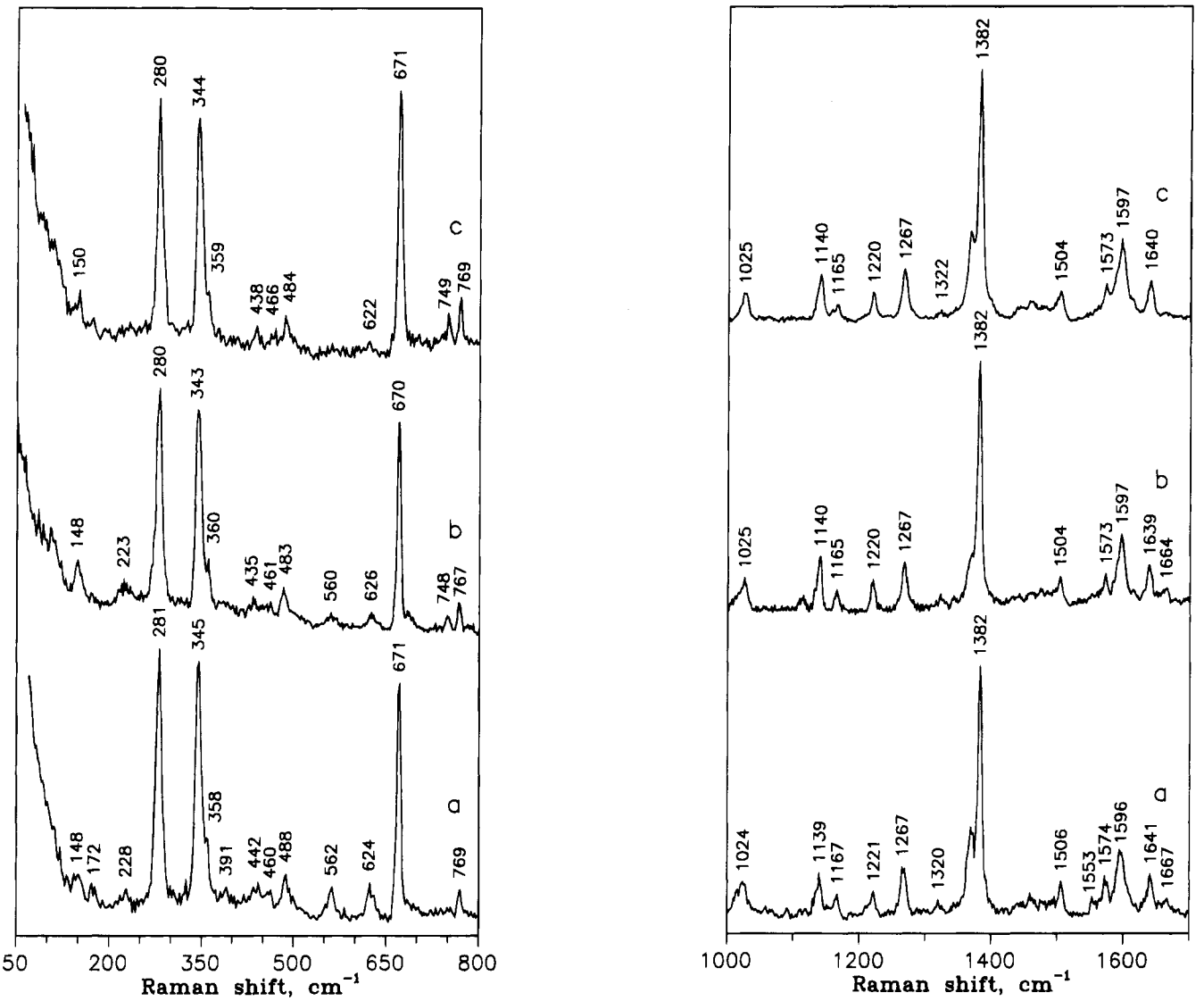

Figure 13. RR spectra of CuOEP in a THF/diethyl ether (1:1) mixture recorded at 77 K (left panel, low-frequency region; right panel, high-frequency region). Excitation wavelengths: (a) 400 nm; (b) 402 nm; (c) 405 nm.

electronic state leads to insignificant perturbation of the porphyrin core structure that is being reflected in rather small shifts of marker Raman bands. On the contrary, the observed large frequency downshifts of marker lines in transient RR and RCARS spectra obtained at high excitation power in O-containing solutions indicate that the porphyrin core substantially expands in the *excited electronic state*. This core expansion presumably accommodates the added electron density in the metal $d_{x^2-y^2}$ orbital due to the promotion of one of the inner d_{z^2} electrons. So, the above-proposed assignment of the photoinduced transient exciplex species to the excited $^2[d_{z^2},d_{x^2-y^2}]$ state is proved to be the most probable.

C. Exciplex Deactivation Pathways. According to previous photophysical studies[4,6-8] and theoretical IEH calculations,[7,14] axial ligation of Cu−porphyrins by σ-donor solvent molecules could lead to a decrease in the energy of the CT $^2[a_{2u},d_{x^2-y^2}]$ state and its active participation in the process of excitation relaxation. However, transient nanosecond Raman and picosecond absorption spectra do not reveal any direct spectral manifestation of this process for Cu−porphyrins in O-containing solvents. Meanwhile, reliable indirect evidence of the existence of an additional exciplex deactivation pathway has been obtained by the saturation RCARS technique.

To extract information on the dynamic behavior of the photoexcited molecule, laser pulses are usually used having a duration comparable to or shorter than the excited-state lifetime. On the contrary, in the saturation technique, transient spectra are recorded under intense radiative saturation of the one-photon transitions involved. The characteristic decay times of metalloporphyrins under investigation lie in the subnanosecond time domain. Therefore it is possible to produce a quasi-stationary distribution of the molecules over the electronic energy levels tracing the temporal profile of the 10 ns laser pulse. As a result, RCARS spectra from the ground and/or excited states can be recorded and the population redistribution over the excited states can be examined as a function of excitation power. In principle, this saturation technique enables one to obtain new information about the relaxation processes, in addition to the data of direct kinetic measurements. For example, in the case if there existed several parallel relaxation channels, the time-resolved technique would monitor the predominant decay pathway, while changes in saturation spectra under variation of the excitation power would reflect also the presence of the other decay pathways. It should also be noted that the saturation RCARS technique is advantageous over saturation spontaneous RR spectroscopy because of the coherent nature of scattering, which results in better spectral resolution, the possibility of polarization separation of near-by lines, better homogeneity of sample illumination, etc.

We have performed a comparative saturation RCARS study for nickel and copper complexes of OEP in THF in which the population of the most long-lived excited (d,d) state resides.

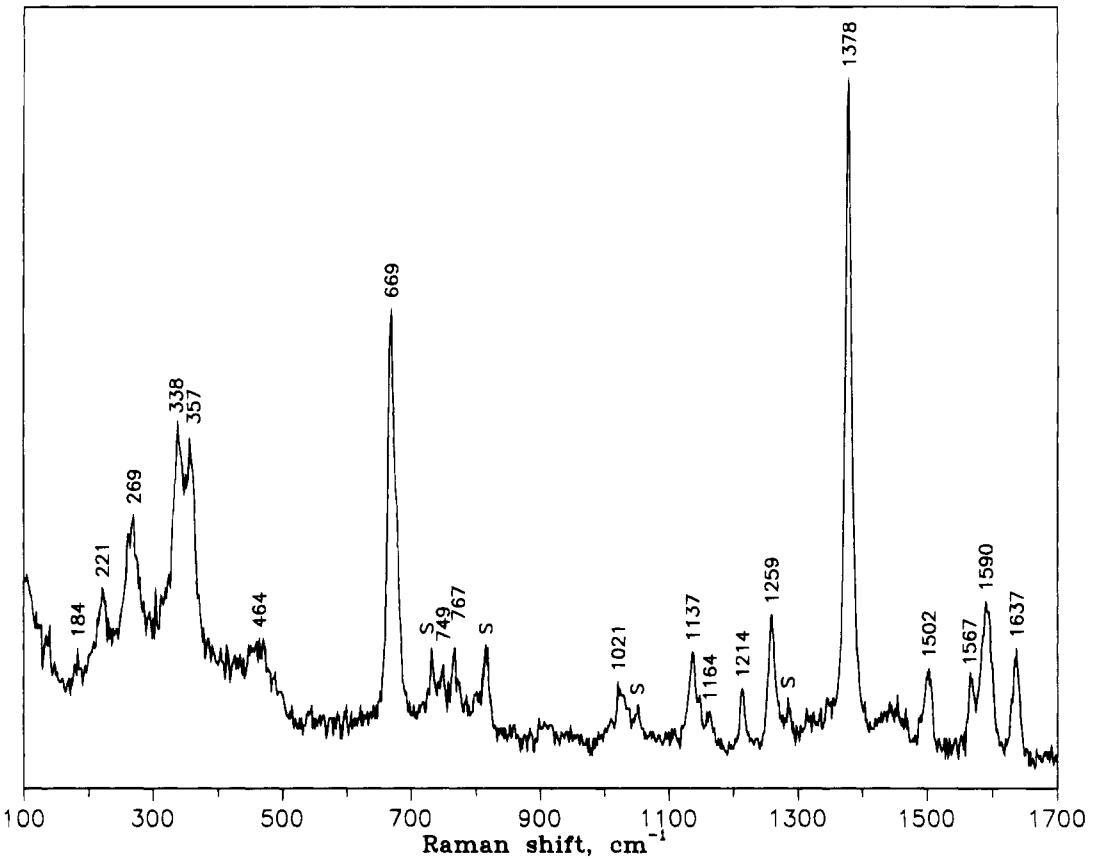

Figure 14. RR spectra of CuOEP in piperidine, recorded with 402 nm excitation. "S" indicates solvent lines.

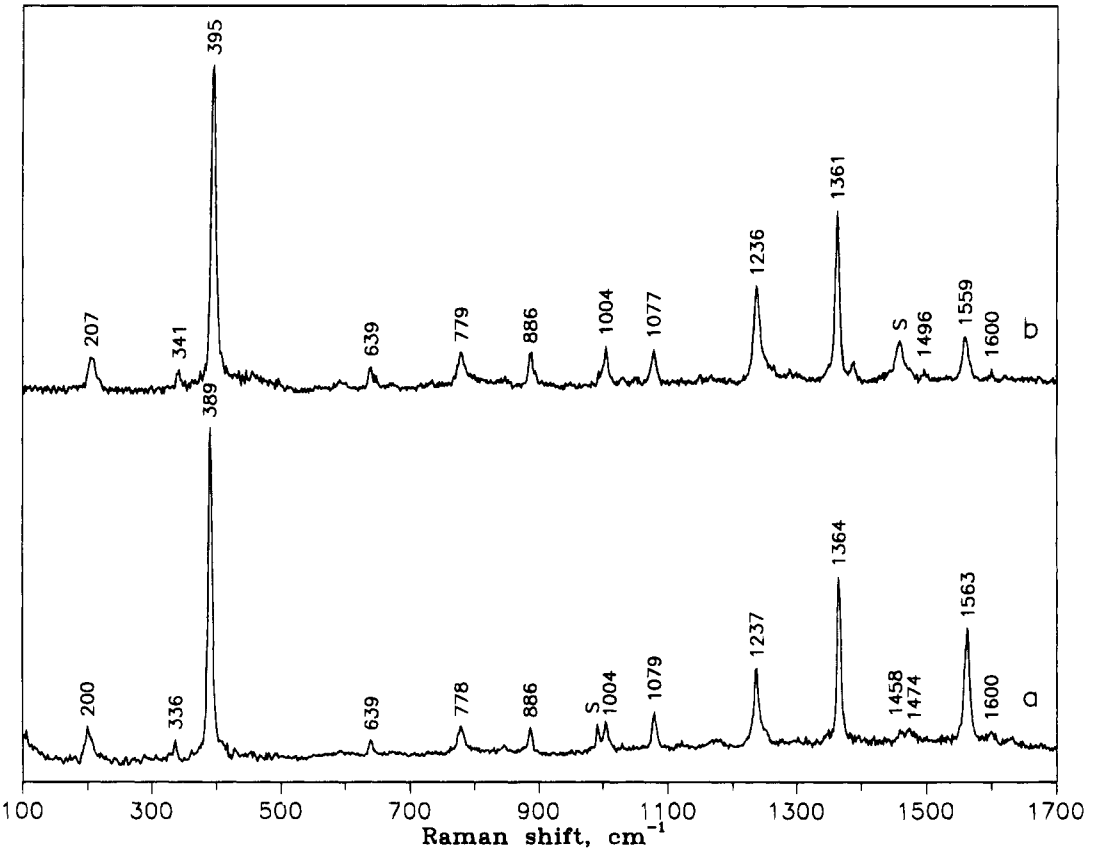

Figure 15. RR spectra of CuTPP in benzene (a) and piperidine (b) solvents, recorded using low-intensity excitation at 402 nm. "S" indicates solvent lines.

The comprehensive description of this RCARS study together with the simulation of the dynamic behavior of the investigated systems using the quasi-stationary rate equations approach will be done in a future paper. Here we restrict ourselves to a qualitative discussion which enables us to make definite conclusions about the exciplex deactivation pathways.

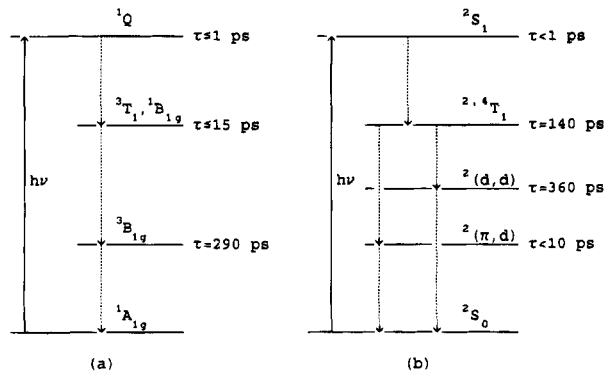

Figure 16. Schematic diagram of electronic energy levels and presumable decay pathways after photoexcitation for NiOEP (a) and CuOEP (b) in THF.

In the case of NiOEP the following results have been obtained (the electronic energy levels diagram for NiOEP is schematically represented in Figure 16a). An increase in the excitation intensity (I_{ex}) leads to an effective transfer of the molecules from the ground $^1A_{1g}$ state to the excited $^3B_{1g}$ state, and at $I_{ex} \approx 10^8$ W/cm^2 complete depopulation of the ground electronic state occurs.[20] Further increase in I_{ex} leads to redistribution of the NiOEP molecules between the excited states, and the second set of transient Raman peaks arises due to the stepwise population of the higher-lying excited $^1B_{1g}$ state. The preliminary results of these studies have been published elsewhere.[26]

For CuOEP, the processes of population redistribution over the excited states with increasing excitation power are quite different from that for NiOEP. The distinctive feature of transient RCARS spectra obtained even at the highest possible nondestructive excitation intensity ($I_{ex} \approx 10^9$ W/cm^2) is the absence of full ground-state depletion. Moreover, the proportion of CuOEP molecules transferred to the excited (d,d) state at a fixed value of excitation power depends on the type of O-containing axial ligand. This is well seen from the spectra given in Figure 4 by the intensities ratio of the lines at ≈1586 cm^{-1} (ground state) and ≈1540 cm^{-1} (excited state).

At the same time, picosecond transient absorption studies reveal that photoinduced absorption changes for nickel and copper OEP complexes dissolved in THF exhibit a similar relaxation behavior. In both complexes double-exponential kinetics of spectral changes is observed: the first (fast) component is associated with the deactivation of the excited triplet (π,π^*) state; the second (slow) component represents decay of the most long-lived excited (d,d) state, namely $^3B_{1g}$ for NiOEP and $^2[d_{z^2},d_{x^2-y^2}]$ for CuOEP. (Note that for NiOEP the first fast relaxation component may also represent the deactivation of the excited $^1B_{1g}$ state[26,38] as well as the vibrational cooling[46] or conformational dynamics.[36]) The lifetimes of the long-lived excited (d,d) state for both complexes are nearly equal: 290 ps for NiOEP in THF[34] and 360 ps for CuOEP in THF.

Taking into account all the above-mentioned facts, it is quite reasonable to assume for the exciplex $[(CuP)^*_{T_1}-L]$ the existence of an additional effective deactivation channel which does not involve the excited (d,d) state. This decay channel hinders complete ground-state depletion; and accumulation of all the Cu−porphyrin molecules in the most long-lived excited (d,d) state does not occur even at the highest excitation power. According to the above discussion, the relaxation via the excited CT state is the most probable pathway for this additional decay process. Since we have not detected any direct spectral evidences of the CT state, it is hardly possible to establish the exact mechanism of its influence on the exciplex deactivation process. Probable here are both the direct CT population in the course of excitation relaxation (if the CT state is downshifted below the triplet-state manifold) and its thermal population (if the CT state becomes close in energy but lies higher than the triplet states). According to IEH calculations, the first assumption is more probable, since it was found[7,14] that binding of a σ-donor molecule by a Cu−porphyrin leads to a more significant decrease in energy of the CT state compared to the (d,d) state, and direct population of the latter in the course of exciplex deactivation is reliably established.

Thus, the full scheme of the photoinduced processes for Cu−porphyrins (CuP) in O-containing solvents (L) can be schematically represented as follows (see also Figure 16b):

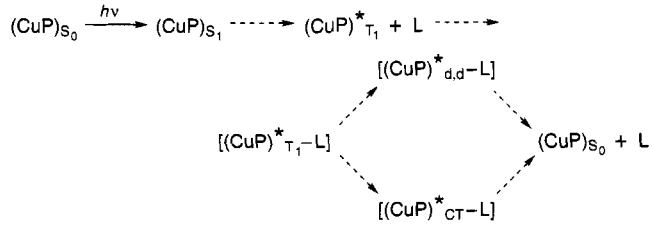

However, IEH calculations systematically underestimate the energies of CT states,[2] so we could not exclude completely the probability for the excited (d,d) state to be lower in energy than the CT state. In any case, the existence of a competition between parallel decay channels via the excited CT and (d,d) states explains well the different percentages of the excited Cu−porphyrin molecules under the same excitation power for a whole set of various O-containing solvents. The monoexponential kinetics of spectral changes for Cu−porphyrins in DMSO and DMF can also be explained by the predomination of the relaxation channel via the CT state. This last case reveals similarity with the process of axial binding by Cu−porphyrins of the molecules of N-containing organic bases.[7]

D. Structural Properties of Five-Coordinate CuOEP Ligated by THF. At last, we discuss the distortions of the Cu−porphyrin structure caused by axial coordination of an O-containing solvent molecule both in the ground state at 77 K and in the excited (d,d) state at ambient temperature on the basis of RR and RCARS data for CuOEP in THF.

1. Ground-State Species at 77 K. It is known that the structure of OEP metallocomplexes in solution at ambient temperature is planar with the ethyl substituents being perpendicular to the porphyrin plane.[47] Depending upon the relative orientations of the eight ethyl groups, two isomeric planar triclinic forms are distinguished (so-called A and B forms).[24b,48] The presence in a solution of both these forms is revealed by the appearance of two pairs of Raman lines corresponding to ν_8 and ν_9 modes in the low-frequency region, which are strongly coupled metal−pyrrole breathing and C_b−ethyl bending motions and exhibit high sensitivity to ethyl orientations.[24b] Recent Raman studies of NiOEP[49,50] have found the presence of the third, namely, ruffled tetragonal conformation in a solution, even at room temperature. This ruffled form manifests itself most clearly in inhomogeneous broadening of the ν_{10} band consisting of the two components at 1660 cm^{-1} for planar and ≈1650 cm^{-1} for ruffled forms.[49] In the low-frequency region of the NiOEP Raman spectrum, several out-of-plane (oop) modes are activated, also indicating that the solution structure is ruffled.[50] Meanwhile, the structure of CuOEP in solution at room temperature is planar,[47] with no evidence of the inhomogeneous broadening of Raman lines due to ruffling.

Our RR studies at liquid nitrogen temperature revealed that, on lowering the temperature of a solution, modes ν_8 and ν_9 become narrower and more intensive (compare spectra in Figures 1 and 13c), indicating the predomination in the vitrified

TABLE 4: Summary of Raman Frequencies and Shifts (cm^{-1}) of the Structure-Sensitive Bands in Spectra of Copper− and Nickel−Porphyrins, Their Cation and Anion Radicals, and Relative Biological Compounds

					ν_{10}		ν_2		ν_{19}		ν_{11}		ν_3		ν_4	
N	compound	ES[a]	CN[b]	ref	ν	$\Delta\nu$	ν	$\Delta\nu$	ν	$\Delta\nu$	ν	$\Delta\nu$	ν	$\Delta\nu$	ν	$\Delta\nu$
1	CuOEP/THF	grd	4	16[c]	1639	−29	1594	−10	1586	−46	1571	−14	1504	−14	1379	−14
	CuOEP/THF	exc	5		1610		1584		1540		1557		1490		1365	
2	CuPPDME/CS_2	grd	4	14	1634	−9			1584	−14			1503	−12	1373	−1
	^{Cu}Cyt-*c*, pH 7	grd	5		1623				1570				1491		1372	
3	CuOEP/CH_2Cl_2	grd	4	40	1636	−5	1591	+19			1563	+37	1502	−5	1378	−18
	$CuOEP^{\bullet+}ClO_4$	grd			1631		1610				1600		1497		1360	
4	NiOEP/THF	grd	4	20,[c] 35c	1655	−29	1601	−16	1603	−41	1577	−13	1519	−25	1383	−8
	NiOEP/THF	exc	4		1626		1585		1562		1564		1494		1375	
5	NiOEP/toluene	grd	4	35c	1657	−28							1522	−26	1385	−5
	NiOEP/toluene	exc	4		1629								1496		1380	
6	NiOEP/CH_2Cl_2	grd	4	45	1655	−43	1600	−14	1602	−43	1575		1519	−39	1382	−12
	NiOEP/pip	grd	6		1612		1586		1559		?		1480		1370	
7	NiPPDME/CH_2Cl_2	grd	4	45	1655	−51	1593	−27	1602	−50	1578	−24	1519	−39	1381	−13
	NiPPDME/pip	grd	6		1604		1566		1552		1554		1480		1368	
8	^{Ni}hemoglobin	grd	4	44	1658	−39	1593	−19					1519	−34	1378	−10
	^{Ni}hemoglobin	grd	5		1619		1574						1485		1368	
9	NiOEP/THF	grd	4	51	1655		1601	−11	1609	−34	1581	−47	1521	−39	1382	−40
	$Ni^{\bullet-}$OEP	grd			?		1590		1575		1534		1482		1342	

[a] ES = electronic state. [b] CN = coordination number. [c] Including Raman data of the present work.

CuOEP sample of one of the isomeric conformations of the triclinic structure, namely, the B form. Thus, excitation of a five-coordinate species [CuOEP−THF] at 405 nm (Figure 13c) gives rise to an RR spectrum corresponding to the planar porphyrin structure. At the same time, as the excitation wavelength decreases, a four-coordinate species is excited as well, and several new Raman bands appear (Figure 13a,b). The most prominent bands are at 228, 562, 624, and 1667 cm^{-1}, which we assign to oop vibrations of the porphyrin skeleton. So, the noncomplexed form of CuOEP, effectively excited at 400 nm, displays clearly in Raman spectra the ruffled structure. An interesting feature of the spectrum taken at 400 nm is the presence of a pronounced nonplanar analog of the ν_{10} mode at a higher frequency of $\approx$1667 cm^{-1}, whereas for NiOEP the ν_{10} mode of the ruffled form exhibits a downshift of 10 cm^{-1}. Our work corroborates earlier studies of Spaulding et al.,[47] where Raman spectra of CuOEP in a KBr pellet contain lines at 1660 and 1638 cm^{-1}, indicating the existence of two molecular forms for CuOEP. So, proceeding from the obtained results, it is possible to assume that binding of an axial ligand stabilizes the planar structure of CuOEP at liquid nitrogen temperature, while the noncomplexed species exists in the ruffled form.

2. Exciplex Species at Ambient Temperature. The characteristic feature of the transient exciplex spectra of CuOEP recorded at ambient temperature (Figures 1−4) is considerable downshifts of core-size and oxidation-state marker lines above 1350 cm^{-1}. Table 4 gives the frequency values of marker bands (ν_i) and their shifts ($\Delta\nu_i$) for the investigated CuOEP exciplex (line 1) and for a number of other copper and nickel porphyrins in the ground and excited states (lines 2 and 4−8) as well as for their cation and anion radicals (lines 3 and 9).

As noted above, the complexation of CuOEP in the ground electronic state is characterized by small shifts of skeletal modes. The largest values of $\Delta\nu$ are observed for copper cytochrome-*c*, pH = 7 (line 2), but even in this case the shift values are much smaller than those observed in transient exciplex spectra (line 1). Raman spectra of the π cation radical $CuOEP^{\bullet+}$ display frequency shifts (line 3) that also differ both in values and signs from the data of our investigations. These facts reveal that the exciplex can be assigned neither to the ground state of the unstable [CuP−L] complex nor to the excited CT state, which is modeled by cation radical spectra.

The best agreement is observed between the shifts of marker line frequencies in transient spectra of CuOEP and of four-coordinate NiOEP from the excited $^3B_{1g}$ state (lines 1 and 4, 5). It should be noted that, on the basis of the available spectral data of previous studies on the excited states of Ni-porphyrins,[20,33−36] it had been impossible to determine the exact values of shifts for several modes (ν_2, ν_{11}). In order to overcome this problem, we have recorded carefully Raman spectra of NiOEP with 416 nm excitation at various power densities (not shown) and, using the subtraction procedure, have obtained a pure high-quality spectrum from the excited (d,d) state.

Six-coordinate high-spin nickel−porphyrins, for which the $^3B_{1g}$ state is the ground electronic state, reveal the largest perturbation of the porphyrin macrocycle.[44,45] The shifts of core-size marker lines in Raman spectra of these complexes (lines 6 and 7) considerably exceed the shift values in the exciplex spectra. Meanwhile, Raman spectra of nickel-reconstituted hemoglobin,[44] which was found to be five-coordinate, display smaller frequency shifts (compare lines 7 and 8 of Table 4), which are closer to the exciplex shift values. These data indirectly support the conclusion that Cu−porphyrins bind in the excited state only one ligand molecule, producing a five-coordinate species.

The distortion of the porphyrin structure due to binding of a σ-donor ligand molecule by the electronically excited Cu−porphyrin manifests itself in two ways. First of all, axial ligation causes the promotion of one of the inner d_{z^2} electrons to the outer half-filled $d_{x^2-y^2}$ orbital with subsequent core expansion in accordance with the increase of the electron radius of the metal. Spaulding et al.[47] first discovered that the frequency of an anomalously polarized Raman band, later assigned as the A_{2g} mode ν_{19},[23] showed a negative linear dependence on the core size. Further investigations[52,53] reported similar correlations for all the skeletal modes above 1450 cm^{-1} being called core-size marker lines. For a given vibrational mode this dependence is described by the expression $\nu = K(A - D)$, where ν is a mode frequency, K and A are the slope and intercept, and $D = C_t - N$ is the porphyrin core size, defined as the distance between the center of the porphyrin ring and the pyrrole nitrogen atoms. Such dependencies have been studied for metallocomplexes of OEP several times,[40a,54,55] but the calculated values of K and A corresponding to the best-fit line through the data points

TABLE 5: Raman Skeletal Mode Frequencies (cm^{-1}) and Core-Size Values (Å) of Metallooctaethylporphyrins, Used For Determination of the Correlation Parameters for the Best-Fit Line to the Frequency versus Core-Size Plots

compound	core size[a]	ν_{10}	ν_2	ν_{19}	ν_{11}	ν_3	refs
$Ni^{II}OEP$	1.958	1655	1601	1603	1576	1519	20,[b] 24b, 47, 56
$Co^{II}OEP$	1.976	1647	1600	1598	1574	1512	40, 56
$Cu^{II}OEP$	2.000	1638	1592	1584	1569	1503	16d,[b] 40, 41b, 47, 56
$Fe^{III}OEP(Br)$	2.019	1629	1581	1568	1559	1493	54
$Zn^{II}OEP$	2.036	1618	1581	1563	1558	1485	40a, 41a, 56
$Fe^{III}OEP(DMSO)_2$	2.045	1612	1573	1553	1551	1483	54

[a] The values of core size were obtained from ref 55 and references therein. The values of Raman frequencies were averaged over the data obtained from the works indicated in the column labeled refs. [b] Including Raman data of the present work.

TABLE 6: Calculated Core-Size Correlation Parameters for High-Frequency Skeletal Modes above 1450 cm^{-1} of Metallooctaethylporphyrin Complexes

parameter[a]	ν_{10}	ν_2	ν_{19}	ν_{11}	ν_3
K	484.9	324.9	581.7	284.3	428.1
A	5.374	6.893	4.719	7.510	5.507

[a] Slope K (cm^{-1}/Å) and intersept A (Å) for the relation $\nu = K(A - D)$, where ν is mode frequency and D is center-to-pyrrole distance (C_t–N).

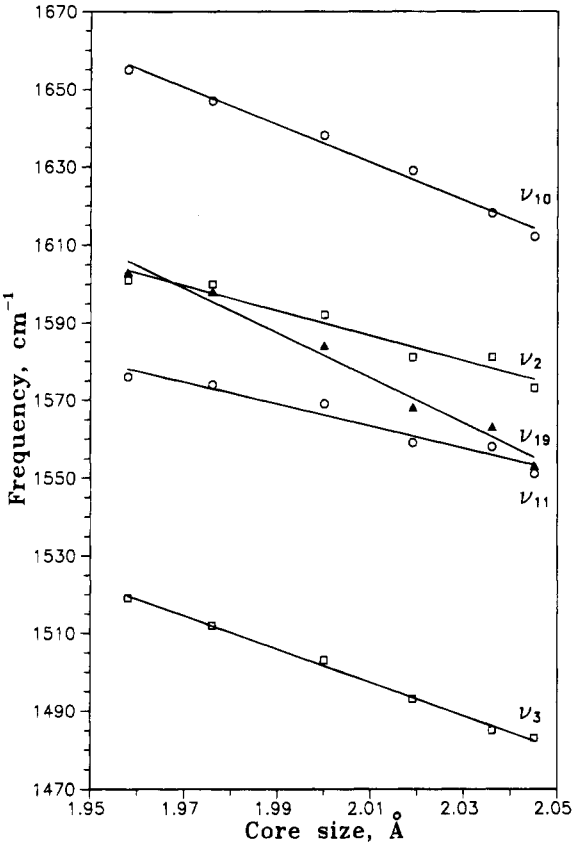

Figure 17. Plots of Raman marker line frequencies against the values of core size for metallooctaethylporphyrin complexes (see Table 5). The solid lines were obtained by linear regression of the data (best-fit parameters of the lines are listed in Table 6).

considerably differ for a number of modes. Therefore, we have also plotted these dependencies proceeding from the crystallographic data base available, literature, and our own data on Raman frequencies of characteristic skeletal modes. The data used in the calculations and the obtained K and A values for a number of core-size marker bands are given in Tables 5 and 6 and are presented in Figure 17. It should be noted that our best-fit core-size correlation parameters were found to be very close to those obtained by Ozaki et al.[54]

Proceeding from the obtained dependencies between the marker line frequencies and core sizes, we estimated the sizes of the porphyrin macrocycles in the excited (d,d) states for nickel and copper OEP complexes (Table 7). For the excited $^3B_{1g}$ state of NiOEP, the spread in values of the porphyrin core size calculated by frequencies of different skeletal modes is rather small with the average value of ≈2.02 Å. In contrast, for the excited $^2[d_{z^2},d_{x^2-y^2}]$ state of the CuOEP exciplex, the values of the core size calculated on the basis of the frequencies of modes ν_{10} and ν_{19} are considerably larger than those calculated on the basis of ν_2, ν_{11}, and ν_3. This result can be accounted for by the assumption that the attachment of an O-containing molecule as an axial ligand to the copper ion causes the removal of the central metal out of the macrocycle plane with the formation of a domed structure. Indeed, as the calculations by Prendergast and Spiro have shown,[55] even a small tilt of the pyrrole rings in a domed porphyrin structure causes considerable frequency downshifts of the ν_{10} and ν_{19} modes, which are both out-of-phase stretching C_aC_m modes and are therefore especially sensitive to oop movement of the C_m atoms. These frequency downshifts, in turn, should lead to the too high values of the core size calculated on the assumption of the linear correlation between ν and D. At the same time the frequencies of other skeletal modes above 1450 cm^{-1} are less sensitive to the oop deformations of the porphyrin skeleton.[55] Therefore, estimations of the porphyrin core size made on the basis of the frequencies of the ν_2, ν_{11}, and ν_3 modes ($D \approx 2.03$ Å) appear to be more precise.

TABLE 7: Values of Core Size (Å) for the Excited (d,d) States of NiOEP and CuOEP, Calculated on the Basis of Marker Line Frequencies (cm^{-1}) Using Parameters Listed in Table 6

compound	mode	frequency[a]	core size
$(NiOEP)^*_{d,d}$	ν_{10}	1626	2.027
	ν_2	1585	2.015
	ν_{19}	1562	2.034
	ν_{11}	1564	2.009
	ν_3	1494	2.017
$[(CuOEP)^*_{d,d}–THF]$	ν_{10}	1610	2.054
	ν_2	1584	2.018
	ν_{19}	1540	2.072
	ν_{11}	1557	2.033
	ν_3	1490	2.027

[a] The values of mode frequencies in the excited state were obtained from refs 20 and 35c and from the present work.

Second, the attachment of an O-containing molecule influences the porphyrin structure also due to the electron density redistribution between the axial ligand and metal orbitals. This redistribution, in turn, leads to a change in the interaction between the metal d_π and the porphyrin e_g^* orbitals and manifests itself mainly in the frequency shift of the ν_4 mode known as the characteristic oxidation state and π electron density marker band.[53,57] The effect is the most pronounced for anion radical complexes of nickel and cobalt porphyrins for which the localization of an additional charge on the d orbitals of the central metal results in the ν_4 mode downshift of ≈40 cm^{-1} (ref 51, line 9 of Table 4). Let us consider from this point of view the structural deformations in the excited (d,d) states of NiOEP and CuOEP. Four-coordinate excited Ni–porphyrin

displays a small downshift ($\Delta\nu = 5-8$ cm^{-1}) of the ν_4 frequency that is being attributed rather to a weak dependence of the value of the ν_4 frequency versus the porphyrin core size[35c,55] than to the appearance of an additional charge on the central metal. This explanation is consistent with the experimental findings that the process of photoinduced population of the excited (d,d) state in four-coordinate Ni−porphyrins is a purely intramolecular process, since it takes place in noncoordinating solvents as well.[35c,36] Transient Raman spectra of the CuOEP exciplex reveal more significant downshifts of the ν_4 mode. Thus, this downshift cannot be explained merely by the effect of the porphyrin core expansion and is indicative of the electron density donation from the oxygen p_z orbital of an axial ligand molecule to the d orbitals of the central metal. Such a change in electron density raises the energy of the $d\pi$ orbitals, increasing the $d_\pi-e_g^*$ overlap. As a result, mode ν_4 exhibits considerable downshifts of 14−16 cm^{-1}.

As concerns spectral changes in other regions of transient Raman spectra of the CuOEP exciplex, we note the absence of or negligible frequency shifts of ethyl substituent deformations (CH_2 wagging at ≈1319 cm^{-1}, CH_2 twisting at 1260 cm^{-1}). Small, up to 6 cm^{-1}, downshifts are observed for CC stretches, namely for the in-phase C_bC_1 stretching mode at ≈1137 cm^{-1} (skeletal mode ν_5) and the out-of-phase C_1C_2 stretching mode at ≈1024 cm^{-1}. This points to the fact that perturbation of the exciplex structure does not affect remarkably the peripheral groups. We also note the considerable strength of the ethyl modes in the exciplex spectra. Moreover, pronounced new bands activate in the 1420−1480 cm^{-1} region which can be assigned to the methylene deformations (CH_2 scissors). These facts could be explained as follows. Spiro et al. have suggested[24b,58] that the enhancement of ethyl modes for NiOEP might be accounted for by the hyperconjugation effect. The out-of-plane orientation of the ethyl substituents places the ethyl σ_π orbitals in the proper orientation to interact with and raise the energy of the porphyrin a_{1u} highest occupied molecular orbital, which has significant electron density on the C_b atoms. Internal motions of the ethyl group, especially stretching of the CC bonds, would modulate this $\sigma_\pi-a_{1u}$ interaction and thereby distort the excited state, leading to resonance enhancement.[58] In the framework of this consideration, it is tempting to assume that the distortion of the porphyrin core due to both doming and expansion facilitates $\sigma_\pi-a_{1u}$ interaction so that not only CC stretching modes but also the methylene deformations are enhanced well in the exciplex RR spectra with excitation at the Soret band.

The ν_7 band at ≈670 cm^{-1}, which was assigned to the breathinglike motion of the 16-membered macrocycle,[23] exhibits in the excited-state spectra small downward frequency shifts and is far less intensive than its ground-state counterpart. This fact corroborates our conclusion that the exciplex structure is domed. Indeed, the perturbation of the flat porphyrin structure causes mixing of the ν_7 mode with the oop modes, and such deviation from breathinglike motion presumably leads to reduction of the ν_7 mode intensity.[23] The similar effect of a decrease in the ν_7 line intensity was observed for domed high-spin Fe−porphyrins.[59]

Also noteworthy is the absence in the exciplex spectrum (Figure 1c) of the prominent Raman bands in the low-frequency region below 500 cm^{-1}. A similar behavior is characteristic of RR spectra of $Ni^{\bullet-}$OEP and $Co^{\bullet-}$OEP monoanions having an additional charge on the metal d orbitals.[51] The nature of this effect is still not clear; we can only suppose the presence of some dynamic effect leading to a significant broadening of the low-frequency modes.

Conclusions

So, in the course of the spectroscopic studies on intermolecular interactions between Cu−porphyrins and O-containing solvent molecules, we have obtained the following results.

(i) The lifetime of the excited tripdoublet−quartet state manifold $^{2,4}T_1$ is dramatically decreased by hundreds of picoseconds, indicating the quenching influence of the solvent environment.

(ii) The quenching is a result of diffusion-controlled binding of an O-containing molecule L as an axial ligand to the excited Cu−porphyrin in the $^{2,4}T_1$ state to form the five-coordinate exciplex $[(CuP)^*_{T_1}-L]$.

(iii) If L = THF, 1,4-dioxane, or cyclohexanone, then the deactivation of the exciplex proceeds mainly via the excited $^2[d_{z^2},d_{x^2-y^2}]$ state having a lifetime of hundreds of picoseconds.

(iv) The competitive decay pathway is revealed in RCARS saturation measurements: deactivation of the triplet-excited exciplex proceeds also via the additional relaxation channel, presumably involving the excited CT state, resulting in an instant release of an axial ligand. In the case of L = DMSO or DMF, this second deactivation channel via the CT state is predominant to a considerable extent.

(v) Transient RR and RCARS spectra of the exciplex species $[(CuOEP)^*_{d,d}-THF]$ at ambient temperature reveal both the significant expansion of the porphyrin core ($D \approx 2.03$ Å) and removal of the central metal out of the macrocycle plane with production of the doming structure. Furthermore, a large frequency downshift of the ν_4 marker line is indicative of the electron density donation from the oxygen p_z orbital of the axial ligand molecule to the d orbitals of central metal. In contrast, low-temperature RR spectra gave experimental evidence that binding of a THF molecule as an axial ligand in the ground state stabilizes the planar structure of CuOEP at liquid nitrogen temperature, while the noncomplexed CuOEP species exists in the ruffled form at 77 K.

The influence of the donor/acceptor properties and dielectric constants of solvents on Cu−porphyrins' excited-state photophysics and structure is a very interesting problem. The question is why the exciplex deactivation proceeds via the excited CT state in N-containing solvents (pyridine, piperidine, pyrrolidine) as well as in O-containing DMF and DMSO (note that DMSO can bind through the S atom as well), while in O-containing THF, dioxane, and cyclohexanone the excited (d,d) state actively participates in the deactivation process. The investigation of this problem is in progress now in our group.

Acknowledgment. The authors would like to thank Dr. A. M. Shulga for supplying porphyrin samples, Drs. R. Gadonas and V. Krasauskas for carrying out some picosecond absorption measurements, and Dr. S. N. Terekhov for stimulating discussions on the vibrational spectra of metalloporphyrins. This work was supported in part by the Fundamental Research Foundation of the Republic of Belarus under Grant No. F22-044.

References and Notes

(1) (a) Gurinovich, G. P.; Sevchenko, A. N.; Solovyov, K. N. *Spectroscopy of Chlorophyll and Related Compounds*; Nauka i Tekhnika: Minsk, 1968; pp 517. (b) Solovyov, K. N.; Gladkov, L. L.; Starukhin, A. S.; Shkirman, S. F. *Spectroscopy of Porphyrins: Vibrational States*; Nauka i Tekhnika: Minsk, 1985; pp 414.

(2) Gouterman, M. In *The Porphyrins*; Dolphin, D., Ed.; Academic Press: New York, 1978; Vol. III, Chapter 1.

(3) (a) Smith, B. E.; Gouterman, M. *Chem. Phys. Lett.* **1968**, *2*, 517. (b) Ake, R. L.; Gouterman, M. *Theor. Chim. Acta* **1969**, *15*, 20. (c) Eastwood, D.; Gouterman, M. *J. Mol. Spectrosc.* **1969**, *30*, 437. (d) Gouterman, M.; Mathies, R. A.; Smith, B. E.; Caughey, W. S. *J. Chem. Phys.* **1970**, *52*, 3795.

(4) Dzhagarov, B. M.; Chirvony, V. S.; Gurinovich, G. P. In *Laser Picosecond Spectroscopy and Photochemistry of Biomolecules*; Letokhov, V. S., Ed.; Adam Hilger: Bristol and Philadelphia, 1987; Chapter 3.

(5) (a) Kobayashi, T.; Huppert, D.; Straub, K. D.; Rentzepis, P. M. *J. Chem. Phys.* **1979**, *70*, 1720. (b) Reynolds, A. H.; Straub, K. D.; Rentzepis, P. M. *Biophys. J.* **1982**, *40*, 27. (c) Straub, K. D.; Rentzepis, P. M. *Biophys. J.* **1983**, *41*, 411a.

(6) (a) Chirvony, V. S.; Dzhagarov, B. M.; Gurinovich, G. P. *Bull. Acad. Sci. USSR, Phys. Ser.* **1984**, *48*, 55. (b) Chirvony, V. S.; Dzhagarov, B. M. *Bull. Acad. Sci. Estonian SSR, Phys.-Mat. Ser.* **1982**, *31*, 129.

(7) Kim, D.; Holten, D.; Gouterman, M. *J. Am. Chem. Soc.* **1984**, *106*, 2793.

(8) Hilinski, E. F.; Straub, K. D.; Rentzepis, P. M. *Chem. Phys. Lett.* **1984**, *111*, 333.

(9) Serpone, N.; Ledon, H.; Netzel, T. *Inorg. Chem.* **1984**, *23*, 454.

(10) Shatwell, R. A.; Gale, R.; McCaffery, A. J.; Sichel, K. *J. Am. Chem. Soc.* **1975**, *97*, 7015.

(11) (a) Noort, M.; Jansen, G.; Canters, G. W.; van der Waals, J. H. *Spectrochim. Acta* **1976**, *32*, 1371. (b) van Dijk, N.; van der Waals, J. H. *Mol. Phys.* **1979**, *38*, 1211. (c) van Dijk, N.; Noort, M.; van der Waals, J. H. *Mol. Phys.* **1979**, *44*, 891. (d) van Dijk, N.; Noort, M.; van der Waals, J. H. *Mol. Phys.* 1979, *44*, 913. (e) van der Poel, W. A. J.; Nuijs, A. M.; van der Waals, J. H. *J. Phys. Chem.* **1986**, *90*, 1537.

(12) (a) Bohandy, J.; Kim, B. F. *J. Chem. Phys.* **1980**, *73*, 5477. (b) Bohandy, J.; Kim, B. F. *J. Chem. Phys.* **1983**, *78*, 4331.

(13) Asano, M.; Kaizu, Y.; Kobayashi, H. *J. Chem. Phys.* **1988**, *89*, 6567.

(14) Shelnutt, J. A.; Straub, K. D.; Rentzepis, P. M.; Gouterman, M.; Davidson, E. R. *Biochemistry* **1984**, *23*, 3946.

(15) Antipas, A.; Dolphin, D.; Gouterman, M.; Johnson, E. C. *J. Am. Chem. Soc.* **1978**, *100*, 7705.

(16) (a) Apanasevich, P. A. *J. Mol. Struct.* **1984**, *115*, 233. (b) Apanasevich, P. A.; Gadonas, R.; Kvach, V. V.; Krasauskas, V.; Orlovich, V. A.; Chirvony, V. S. *Khim. Fiz.* **1988**, *7*, 21. (c) Apanasevich, P. A.; Gadonas, R.; Kvach, V. V.; Krasauskas, V.; Kruglik, S. G.; Orlovich, V. A.; Chirvony, V. S. *Bull. Acad. Sci. USSR, Phys. Ser.* **1988**, *52*, 42. (d) Apanasevich, P. A.; Chirvony, V. S.; Kruglik, S. G.; Kvach, V. V.; Orlovich, V. A. In *Laser Applications in Life Sciences*; Akhmanov, S. A., Poroshina, M. Yu., Eds.; SPIE: Bellingham, 1991; Vol. 1403, Part I, pp 195−211.

(17) (a) Apanasevich, P. A.; Kvach, V. V.; Koptev, V. G.; Orlovich, V. A.; Stavrov, A. A.; Shkadarevich, A. P. *Kvantovaya Elektron.* **1987**, *14*, 265. (b) Andreev, S. P.; Antonov, E. V.; Bagdasarov, H. S.; Kvach, V. V.; Kruglik, S. G.; Mikhalenko,Yu. I.; Orlovich,V. A.; Fedorov, E. A. *Zh. Prikl. Spektrosk.* **1989**, *51*, 757.

(18) Apanasevich, P. A.; D'yakov, Yu. E.; Kotaev, G. G.; Kruglik, S. G.; Nikitin, S.Yu.; Orlovich, V. A. *Laser Phys.* **1993**, *3*, 131.

(19) Akhmanov, S. A.; Koroteev, N. I. *Methods of Nonlinear Optics in the Spectroscopy of Light Scattering*; Nauka: Moscow, 1981; pp 543.

(20) Apanasevich, P. A.; Kvach, V. V.; Orlovich, V. A. *J. Raman Spectrosc.* **1989**, *20*, 125.

(21) Gadonas, R.; Danelus, R.; Piskarskas, A. *Kvantovaya Elektron.* **1981**, *8*, 669.

(22) Apanasevich, P. A.; Kvach, V. V.; Orlovich, V. A. *Zh. Prikl. Spektrosk.* **1989**, *50*, 460.

(23) Abe, M.; Kitagawa, T.; Kyogoku, Y. *J. Chem. Phys.* **1978**, *69*, 4526.

(24) (a) Li, X.-Y.; Czernuszewicz, R. S.; Kincaid, J. R.; Su, Y. O.; Spiro, T. G. *J. Phys. Chem.* **1990**, *94*, 31. (b) Li, X.-Y.; Czernuszewicz, R. S.; Kincaid, J. R.; Stein, P.; Spiro, T. G. *J. Phys. Chem.* **1990**, *94*, 47. (c) Li, X.-Y.; Czernuszewicz, R. S.; Kincaid, J. R.; Spiro, T. G. *J. Am. Chem. Soc.* **1989**, *111*, 7012.

(25) (a) Gladkov, L. L.; Solovyov, K. N. *Spectrochim. Acta* **1985**, *41A*, 1437. (b) Gladkov, L. L.; Solovyov, K. N. *Spectrochim. Acta* **1985**, *41A*, 1443. (c) Gladkov, L. L.; Solovyov, K. N. *Spectrochim. Acta* **1986**, *42A*, 1.

(26) Apanasevich, P. A.; Kruglik, S. G.; Kvach, V. V.; Orlovich, V. A. In *Time-Resolved Vibrational Spectroscopy V;* Takahashi, H., Ed.; Springer Proceedings in Physics, Vol. 68; Springer-Verlag: 1992; pp 105−108.

(27) Walters, V. A.; de Paula, J. C.; Babcock, G. T.; Leroi, G. E. *J. Am. Chem. Soc.* **1989**, *111*, 8300.

(28) Reed, R. A.; Purrello, R.; Prendergast, K.; Spiro, T. G. *J. Phys. Chem.* **1991**, *95*, 9720.

(29) Asano, M.; Sato, S.; Kitagawa, T. In *Time-Resolved Vibrational Spectroscopy V*; Takahashi, H., Ed.; Springer Proceedings in Physics, Vol. 68; Springer-Verlag: 1992; pp 111−112.

(30) Kumble, R.; Hu, S.; Loppnow, G. R.; Vitols, S. E.; Spiro, T. G. *J. Phys. Chem.* **1993**, *97*, 10521.

(31) (a) Sato, S.; Asano-Someda, M.; Kitagawa, T. *Chem. Phys. Lett.* **1992**, *189*, 443. (b) de Paula, J. C.; Walters, V. A.; Nutaitis, C.; Lind, J.; Hall, K. *J. Phys. Chem.* **1992**, *96*, 10591.

(32) Rodrigues, J.; Kirmaier, C.; Holten, D. *J. Am. Chem. Soc.* **1989**, *111*, 6500.

(33) Apanasevich, P. A.; Kvach, V. V.; Kozich, V. P.; Orlovich, V. A.; Churkin, A. V. *Opt. Spektrosk.* **1985**, *58*, 488.

(34) (a) Kamalov, V. F.; Kvach, V. V.; Koroteev, N. I.; Toleutaev, B. N.; Chikishev, A. Yu.; Shkurinov, A. P. *JETP Lett.* **1987**, *45*, 87. (b) Chikishev, A. Yu.; Kamalov, V. F.; Koroteev, N. I.; Kvach, V. V.; Shkurinov, A. P.; Toleutaev, B. N. *Chem. Phys. Lett.* **1988**, *144*, 90.

(35) (a) Findsen, E. W.; Shelnutt, J. A.; Friedman, J. M.; Ondrias, M. R. *Chem. Phys. Lett.* **1986**, *126*, 465. (b) Findsen, E. W.; Alston, K.; Shelnutt, J. A.; Ondrias, M. R. *J. Am. Chem. Soc.* **1986**, *108*, 4009. (c) Findsen, E. W.; Shelnutt, J. A.; Ondrias, M. R. *J. Phys. Chem.* **1988**, *92*, 307.

(36) Courtney, S. H.; Jedju, T. M.; Friedman, J. M.; Alden, R. G.; Ondrias, M. R. *Chem. Phys. Lett.* **1989**, *164*, 39.

(37) Chirvony, V. S.; Dzhagarov, B. M.; Timinskii, Yu. V.; Gurinovich, G. P. *Chem. Phys. Lett.* **1980**, *70*, 79.

(38) (a) Kim, D.; Kirmaier, C.; Holten, D. *Chem. Phys.* **1983**, *75*, 305. (b) Kim, D.; Holten, D. *Chem. Phys. Lett.* **1983**, *98*, 584.

(39) (a) Tait, C. D.; Holten, D.; Gouterman, M. *Chem. Phys. Lett.* **1983**, *100*, 268. (b) Tait, C. D.; Holten, D.; Gouterman, M. *J. Am. Chem. Soc.* **1984**, *206*, 6653.

(40) (a) Oertling, W. A.; Salehi, A.; Chung, Y. C.; Leroi, G. E.; Chang, C. K.; Babcock, G. T. *J. Phys. Chem.* **1987**, *91*, 5887. (b) Oertling, W. A.; Salehi, A.; Chang, C. K.; Babcock, G. T. *J. Phys. Chem.* **1989**, *93*, 1311.

(41) (a) Kim, D.; Miller, L. A.; Rakhit, G.; Spiro, T. G. *J. Phys. Chem.* **1986**, *90*, 3320. (b) Czernuszewicz, R. S.; Macor K. A.; Li, X.-Y.; Kincaid, J. R.; Spiro, T. G. *J. Am. Chem. Soc.* **1989**, *111*, 3860.

(42) Yamaguchi, H.; Nakano, M.; Itoh, K. *Chem. Lett.* **1982**, 1397.

(43) Tait, C. D.; Holten, D.; Barley, M. H.; Dolphin, D.; James, B. R. *J. Am. Chem. Soc.* **1985**, *107*, 1930.

(44) Shelnutt, J. A.; Alston, K.; Ho, J.-Y.; Yu, N.-T.; Yamamoto, T.; Rifkind, J. M. *Biochemistry* **1986**, *25*, 620.

(45) Kim, D.; Su, Y. O.; Spiro, T. G. *Inorg. Chem.* **1986**, *25*, 3988.

(46) (a) Rodriguez, J.; Holten, D. *J. Chem. Phys.* **1989**, *91*, 3525. (b) Rodriguez, J.; Kirmaier, C.; Holten, D. *J. Chem. Phys.* **1991**, *94*, 6020.

(47) Spaulding, L. D.; Chang, C. C.; Yu, N.-T.; Felton, R. H. *J. Am. Chem. Soc.* **1975**, *97*, 2517.

(48) Brennan, T. D.; Scheidt, W. R.; Shelnutt, J. A. *J. Am. Chem. Soc.* **1988**, *110*, 3919.

(49) Alden, R. G.; Crawford, B. A.; Doolen, R.; Ondrias, M. R.; Shelnutt, J. A. *J. Am. Chem. Soc.* **1989**, *111*, 2070.

(50) Czernuszewicz, R. S.; Li, X.-Y.; Spiro, T. G. *J. Am. Chem. Soc.* **1989**, *111*, 7024.

(51) Terekhov, S. N.; Ksenofontova, N. M.; Gurinovich, I. F. *Zh. Prikl. Spektrosk.* **1990**, *53*, 576

(52) (a) Choi, S.; Spiro, T. G.; Langry, K. C.; Smith, K. M.; Budd, D. L.; La Mar, G. N. *J. Am. Chem. Soc.* **1982**, *104*, 4345. (b) Parthasarathi, N.; Hansen, C.; Yamaguchi, S.; Spiro, T. G. *J. Am. Chem. Soc.* **1987**, *109*, 3865.

(53) Spiro, T. G.; Li, X.-Y. *Biological Applications of Raman Spectroscopy*; Wiley: New York, 1988; Vol. III, Chapter 1, pp 2−37.

(54) Ozaki, Y.; Iriyama, K.; Ogoshi, T.; Kitagawa, T. *J. Phys. Chem.* **1986**, *90*, 6105.

(55) Prendergast, K.; Spiro, T. G. *J. Am. Chem. Soc.* **1992**, *114*, 3793.

(56) Kitagawa, T.; Ogoshi, H.; Watanabe, E.; Yoshida, Z. *J. Phys. Chem.* **1975**, *79*, 2629.

(57) Spiro, T. G.; Strekas, T. C. *J. Am. Chem. Soc.* **1974**, *96*, 338.

(58) Spiro, T. G.; Czernuszewicz, R. S.; Li, X.-Y. *Coord. Chem. Rev.* **1990**, *100*, 541.

(59) Kitagawa, T.; Abe, M.; Kyogoku, Y.; Ogoshi, H.; Watanabe, E.; Yoshida, Z. *J. Phys. Chem.* **1976**, *80*, 1181.

JP940344+